Parameter and climate data uncertainty as important as climate change for future changes in boreal hydrology

Adrienne M. Marshall[1†], Timothy E. Link[1], Gerald N. Flerchinger[2], Melissa S. Lucash[3]

[1]Department of Forest, Rangeland, and Fire Sciences, University of Idaho, 875 Perimeter Drive, Moscow, ID 83844, USA. [2]USDA Agricultural Research Service Northwest Watershed Research Center, 251 E. Front Street, Suite 400, Boise, ID 83702, USA. [3]Department of Geography, University of Oregon, 1251 University Oregon, Eugene, OR 97403, USA

Corresponding author: Adrienne Marshall (adriennemarshall@gatech.edu)

†Current affiliation: School of Civil and Environmental Engineering, Georgia Institute of Technology, 790 Atlantic Dr. NW, Atlanta, CA 30332, USA

Key Points:

- Summer soil moisture at rooting depth is most sensitive to soil and plant hydraulic parameters and parameter interactions.
- Parameter uncertainty affects magnitude and sign of projected change in ET and θ_{VWC}; similar effect size to climate change and GCM.
- We present parameter values useful for hydrologic modeling in multiple boreal forest types while recognizing equifinality.

Abstract

Soil moisture and evapotranspiration (ET) are important components of boreal forest hydrology that affect ecological processes and land-atmosphere feedbacks. Future trends in soil moisture in particular are uncertain. Therefore, accurate modeling of these fluxes and understanding of concomitant sources of uncertainty are critical. Here, we conduct a global sensitivity analysis, Monte Carlo parameterization, and analysis of parameter uncertainty and its contributions to future soil moisture and ET uncertainty using a physically-based ecohydrologic model in multiple boreal forest types. Soil and plant hydraulic parameters and LAI have the largest effects on summer soil moisture at two contrasting sites. We report best estimates and uncertainty of these parameters via a multi-site Generalized Likelihood Uncertainty Estimation approach. In future scenario simulations, parameter and global climate model (GCM) choice influence projected changes in soil moisture and evapotranspiration as much as the projected effects of climate change in a late-century, high-emissions scenario, though the relative effect of parameters, GCM, and climate vary between objective and study site. Saturated volumetric water content and sensitivity of stomatal conductance to vapor pressure deficit have the most statistically significant effects on change in evapotranspiration and soil moisture, though there is considerable variability between sites and GCMs. In concert, the results of this study provide estimates of: (1) parameter importance and statistical significance for soil moisture modeling, (2) parameter values for physically-based soil-vegetation-atmosphere transfer models in multiple boreal forest types, and (3) the contributions of uncertainty in these parameters to soil moisture and evapotranspiration uncertainty in future climates.

1 Introduction

Future changes in soil water content (θ_{VWC}) in boreal environments are extremely important and quite uncertain. Soil moisture dynamics interact with water table depths and thaw dynamics to influence growth, wildfire spread (Bartsch et al., 2009), and net ecosystem carbon dynamics in both coniferous (Dunn et al., 2007; Krishnan et al., 2008) and deciduous forest types (Cahoon et al., 2018; Yarie & van Cleve, 2010). θ_{VWC} also influences soil temperature and permafrost degradation via increased soil latent heat of fusion and soil thermal conductivity in wetter soils (Subin et al., 2012). Despite this importance, considerable uncertainty remains: hydrologic models project a wide range of potential future θ_{VWC} in Arctic regions primarily due to differences in moisture partitioning between models (Andresen et al., 2020) and θ_{VWC} has been identified as a crucial missing piece of modeling Arctic and boreal ecosystem dynamics (Fisher et al., 2018). This is perhaps to be expected, given a variety of potential competing mechanisms: for example, permafrost thaw and snowpack decreases could lead to soil drying (Lader et al., 2020; Teufel & Sushama, 2019), while projected increases in rainfall could increase θ_{VWC} (Lader et al., 2017). Changes in evapotranspiration (ET) due to altered vapor pressure deficit also influence θ_{VWC}, with potential feedbacks in cases where θ_{VWC} limits ET (Helbig et al., 2020).

Given these competing mechanisms, process-based hydrologic modeling is an important tool for understanding future changes in boreal soil moisture. However, process-based hydrologic models often suffer from equifinality (Beven, 2006). Sensitivity and uncertainty analyses have emerged as tools to understand and constrain the consequences of equifinality by identifying the parameters to which models are most sensitive and assessing the range of variability in model outputs (Pianosi et al., 2016; Wilby, 2005). Global sensitivity analysis methods that explicitly account for interactions between parameters, as opposed to those that rely on modifications of parameters one at a time, are important for comprehensively characterizing model sensitivity (Saltelli et al., 2019). However, these methods can be computationally expensive. The Hilbert-Schmidt Independence Criterion (HSIC) is one approach originating from the machine learning literature that appears to be particularly useful for sensitivity analyses of computationally expensive models with large numbers of parameters (Da Veiga, 2015; Iooss & Lemaître, 2015). Essentially, the HSIC provides an estimate of the dependence of a model outcome on individual input parameters. For estimating model parameter values and associated uncertainty, Generalized Likelihood Uncertainty Estimation (GLUE) methods are a common hydrologic modeling approach favored for their flexibility, relative ease of use, and potential to take advantage of highly parallel computing environments (Beven & Binley, 1992, 2014). GLUE methods require a modeler to specify prior distributions of parameters, generate parameter sets from those distributions, run the model with each parameter set, and identify the parameter sets that result in acceptable model results in comparison with data, which are often deemed “behavioral” in the GLUE parlance.

Sensitivity and uncertainty analyses have been used to assess the relative contributions of parameter selection, climate model selection, and model structure to hydrologic model outcomes, with varied results. For example, several studies in temperate and mediterranean regions have found that parameter selection is a relatively small source of uncertainty relative to climate input data and hydrologic model structure in streamflow simulations (Chegwidden et al., 2019; Dobler et al., 2012; Feng & Beighley, 2020). A study using a monthly water balance model in 61 basins within the Ohio River watershed found that global climate model choice was a more important source of uncertainty for runoff projections, but multi-parameter ensemble uncertainty was more important for soil moisture and groundwater (Her et al., 2019). In another study, uncertainty due to model structure versus climate inputs were of comparable magnitude (Ludwig et al., 2009). In the Colorado River headwaters, choice of calibration data and objective function had a larger effect than choice of hydrologic model on discharge uncertainty (Mendoza et al., 2016). In Arctic regions, Harp et al. (2016) determined that uncertainty in soil hydraulic parameters is a major contributor to future uncertainty in permafrost dynamics, though contributions from climate model uncertainty are even greater. This array of findings suggests that relative importance of different sources of uncertainty depends on geographic context, response variable, model structure, and methodological decisions made by modelers. No such studies to our knowledge have been conducted for soil moisture and ET in boreal regions with discontinuous permafrost.

In this study, we provide a detailed sensitivity and uncertainty analysis of soil moisture and ET using the Simultaneous Heat and Water (SHAW) model in multiple boreal forest types in order to improve ecohydrologic modeling in this critically important region. Specifically, we (1) identify and rank the sensitivity of modeled soil moisture to SHAW parameters and compare them across forest types, (2) implement an automated calibration procedure to identify parameter values that are transferable across years and forest types, and (3) estimate the effects of calibration-constrained parameter uncertainty on uncertainty of future soil moisture relative to GCM choice and the projected effect of climate change. The results will be useful to those who are interested in understanding and reducing uncertainty in future projections through additional field data collection or focused modeling efforts to improve parameter identifiability. These results will also provide further information about the extent to which efforts to constrain future hydrologic uncertainty should focus on parameter or input data uncertainty, and provide new understanding of how specific parameterization choices affect projections of future conditions.

2 Materials and Methods

2.1 Study sites

In this study, we use data from four previously established field sites that represent two upland birch-dominated sites in different stages of post-fire successional trajectories (US-Rpf and UP1A) and two mature spruce forests underlain by permafrost (Smith Lake 1, 2; Figure 1). These sites were selected based on the diversity of forest structure and ecological conditions, data availability for model forcing and evaluation, and minimization of net lateral hydrologic fluxes by focusing on upland environments (Table 1).

Input climate data sources varied between sites depending on availability. Data for the birch-dominated UP1A was obtained from the Bonanza Creek Long-Term Ecological Research (BNZ LTER) site and described in detail in Marshall et al. (2020). Briefly, collocated hourly air temperature, relative humidity, and wind speed data were obtained and gap filled using correlations with data from nearby weather stations. Downward shortwave radiation was obtained from the US-Uaf AmeriFlux site (Iwata et al., 2010; Ueyama et al., 2009). SHAW corrects shortwave radiation for slope and aspect, minimizing the importance of these differences between sites. Precipitation data was obtained from the LTER1 site, 1 km away from UP1A. US-Rpf is an Ameriflux site dominated by birch with all meteorological variables collected except for winter precipitation. Lacking winter precipitation observations, we used snow depth data from the nearby US-Prr AmeriFlux site and estimated liquid water content of new snow accumulation based on the internal algorithm for newly fallen snow density used in SHAW (Anderson, 1976). Soil moisture used for calibration was available at all sites, though depths differed between sites.

Table 1. Characteristics of the four study sites. Vegetation ages refer to age at the start of the study period. Mean annual temperature (MAT) and mean annual precipitation (MAP) are calculated based on our gap-filled dataset over the years included in the study.

Name	**Data source**	**Years**	**Vegetation type**	**Soils**	**Slope (%)**	**Aspect**	**Elevation (m)**	**Lat, Lon (°)**	**MAT (°C)**	**MAP (mm)**
UP1A	BNZ LTER	2003-2015	20-year old birch	Silt loam	15	S	258	64.73, -148.30	-1.2	341
US-Rpf	Ameri-Flux	2011-2018	7-year old birch	2 cm organic; sandy loam	15	NE	497	65.12, -147.43	-0.2	453
Smith Lake 1	GIPL; Ameri-Flux	2007-2018	Mature black and white spruce	20 cm organic; silt loam	6	S	160	64.87, -147.86	-2.9	321
Smith Lake 2	GIPL; Ameri-Flux	2007-2018	Mature black spruce	35 cm organic; silt loam	2	N	157	64.87, -147.86	-2.9	321

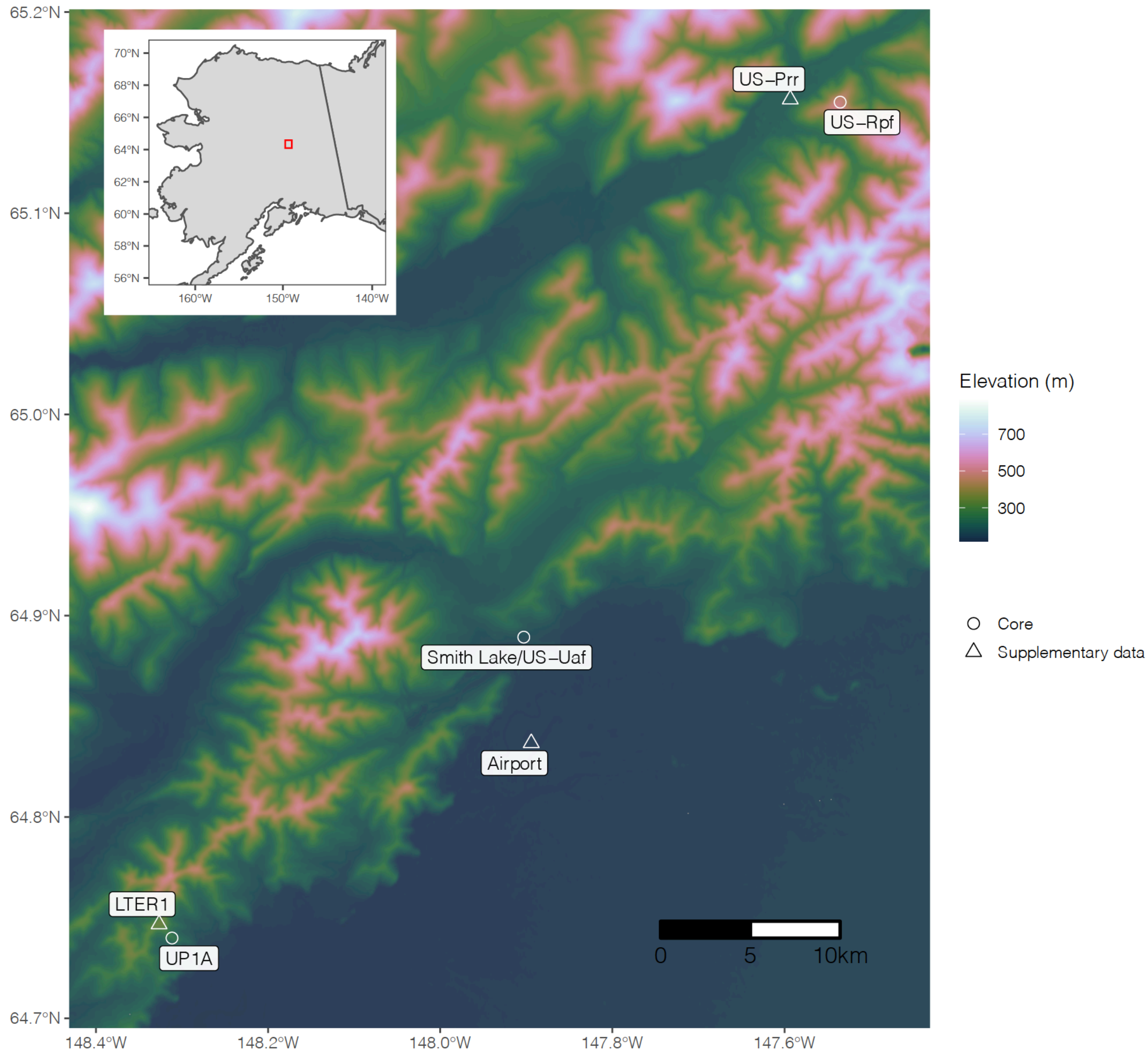

Figure 1. Study area map, showing core sites for study as well as those used for gap-filling and data supplementation. Red square in the inset shows extent of the larger map.

The two spruce sites are Smith Lake 1 and Smith Lake 2, both located on the University of Alaska Fairbanks campus and adjacent to the US-Uaf AmeriFlux site. Hourly air temperature, relative humidity, windspeed, and downward shortwave radiation from the AmeriFlux site were used as climate forcings for simulations of both sites. Minimal gap filling was required for air temperature and relative humidity; in each case, one 39-hour period was missing, and data from the previous two days was substituted. In contrast, 27% of the wind data was missing. We filled gaps using a linear interpolation for missing periods less than 6 hours (5% of data), then used a linear regression against colocated wind sensors (at different heights) at the same site for the rest of the missing periods. Daily precipitation data was obtained from the Fairbanks Airport weather station (Menne et al., 2012), which is approximately 5 km to the south. We disaggregated precipitation data to an hourly time step by estimating the number of precipitating hours per day on wet days at the LTER1 weather station (3 hours). We then randomly sampled 3 hours on each wet day and evenly distributed the daily precipitation values over those hours.

The different sites had varying levels of detail for available vegetation data. Vegetation data for US-Rpf is described in detail in Ueyama et al. (2019), with annual estimates of peak LAI, leaf-on and leaf-off dates, and vegetation height. We estimated biomass for this site based on these data using the allometric equations in Yarie et al. (2007). At UP1A, vegetation surveys provided estimates of stem density and DBH; we estimated biomass and height again following Yarie et al. (2007). The Smith Lake sites have LAI of approximately 2.0 (Iwata et al., 2011) with an 8 m canopy height (Heijmans et al., 2004). Biomass estimates were not available, and were estimated based on relevant literature (Table 2). While this suggests considerable uncertainty in biomass estimates, biomass primarily controls the heat balance of the vegetation layer in SHAW, with minimal effects on hydrology.

Soil textural data was also obtained from different sources for each site. At UP1A, soil texture was determined based on four soil pits (Yarie, 1998). At US-Rpf, post-burn soils have a 2 cm organic layer, underlain by sandy loams (Ueyama et al., 2019) In the Smith Lake area, organic layer depths were obtained by field observations (*personal communication, Vladimir Romanovsky*), and are underlain by silt loams (NCSS, 2020).

2.2 SHAW model

SHAW is a one-dimensional hydrologic model that simultaneously solves the energy and water balance through the atmosphere-vegetation-snow-soil continuum, with a multi-layer plant canopy, snowpack, and soil profile (Flerchinger, 2017; Flerchinger & Saxton, 1989; Link et al., 2004; Figure 2). SHAW inputs include detailed hourly-to-daily climate data, site characteristics, soil texture and layering, soil and plant hydraulic parameters, and parameters for energy balance-based snow accumulation and ablation (Table 2). Outputs include a complete energy and water balance, snowpack dynamics, and soil liquid and frozen water content and temperature at each user-defined node in the soil water profile. The timestep is user-defined, and was hourly in this study. SHAW was initially developed in part to simulate soil moisture dynamics in dynamically freezing soils (Flerchinger et al., 2006; Flerchinger & Saxton, 1989). While this development was based in temperate regions, this feature makes it particularly attractive for modeling in discontinuous permafrost regions. SHAW has previously been applied successfully in boreal and permafrost sites (Marshall et al., 2020; Zhang et al., 2010, 2013).

2.3 Sensitivity analysis

We conducted a global sensitivity analysis of the SHAW model at the burned regenerating birch site and one of the permafrost-underlain spruce sites using the HSIC (Da Veiga, 2015; Iooss & Lemaître, 2015). These two sites were selected to assess sensitivity of soil moisture and evapotranspiration simulations at two contrasting sites. HSIC uses a distance correlation to measure the dependence between an input variable and output variable; it is designed to identify nonlinear dependencies and parameter interactions. Ranges for each parameter were assessed based on literature and available data (Table 2). For a few parameters that are well-defined at each site, such as aspect, the complete possible range was used in order to determine the general importance of these parameters. At each site, 2000 parameter sets were identified using a Latin Hypercube Sampling (LHS) approach with the 'lhs' package in R (Carnell, 2019). The model was run over the calibration period with each parameter set. Average growing season (May-September) soil moisture at the presumed rooting depth for the dominant vegetation at each site (20 cm for black spruce; 60 cm for birch) was calculated for each parameter set. The "sensitivity" package was used to conduct the HSIC sensitivity analysis using universal gaussian kernels and an asymptotic estimation of the p-value (Iooss et al., 2020). When many statistical significance tests are conducted, false discovery rates can be quite high; we followed the method described by Wilks (2016) to identify a p-value that controls the false discovery rate at 10% based on the distribution of p-values obtained from a set of significance tests. This resulted in effective critical p-values of 0.016 at the mature spruce site and 0.034 at the burned site.

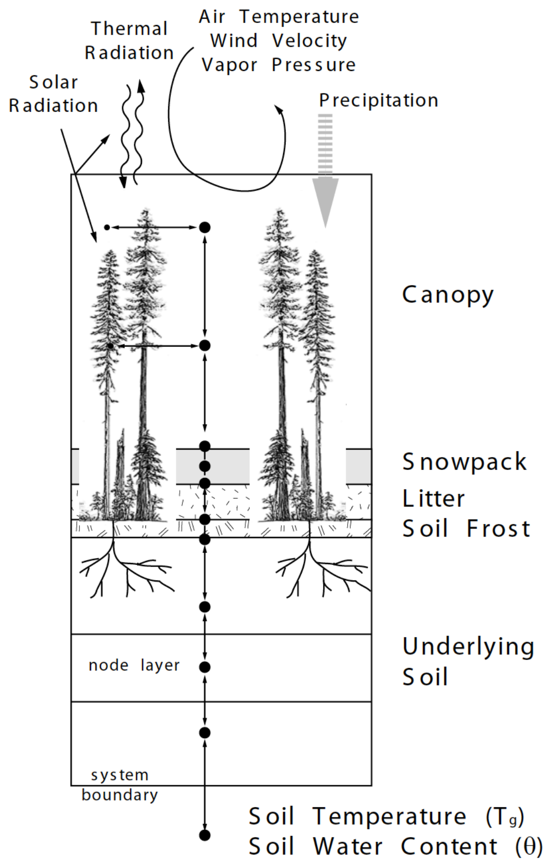

Figure 2. Conceptual diagram of the SHAW model; originally published in Link et al. (2004). Tree illustrations from Van Pelt (2007). © American Meteorological Society. Used with permission.

2.4 Multi-site parameter estimation

We developed a multi-site framework for estimating regional parameters. Parameters that were determined to be statistically significant in the sensitivity analysis were calibrated using GLUE; the others were estimated based on literature values or known values for the site (Table 2). Results indicated that soil hydraulic parameters were significant in some layers but not others; values for all layers were calibrated for consistency. Parameters that described vegetation water use characteristics, such as minimum stomatal conductance and Jarvis-Stewart environmental feedback parameters, were assumed constant within vegetation types but variable between vegetation types. Organic soil hydraulic parameters were assumed constant between all organic soils in the study. A three-layer mineral soil profile was delineated from 0-20 cm, 20-80 cm, and 80-600 cm. Sites with an organic layer used the organic layer, followed by the second and third mineral layers. Requiring soil hydraulic parameters to remain constant between sites is likely an oversimplification, but lacking a basis on which to systematically vary soil hydraulic parameters within the SHAW framework, this approach was selected to ensure a reasonably simple and consistent parameterization between sites.

A GLUE methodology was used to calibrate the sensitive model parameters. We used LHS sampling with the parameters that were determined by the sensitivity analysis to significantly affect growing season soil moisture. In order to ensure plausible relationships of parameters between soil layers, specifically K_{sat} and θ_{sat} decreasing with depth and bulk density increasing with depth in mineral soils, we sampled $5x10^6$ parameter sets, then selected only those that met these criteria, resulting in 22664 parameter sets used in the GLUE method. All parameter sets were run over the first seven years of data available at each site as a calibration period, and daily θ_{VWC} RMSE at the depth with observations closest to presumed rooting depth was evaluated over the May-September growing season. To include evapotranspiration in the parameter selection criteria, we also evaluated the mean absolute error of growing season total evapotranspiration (MAE ET) at the two sites that had observed latent heat fluxes. Results indicated that RMSE of VWC at Smith Lake 2 was particularly poor with all parameter sets, suggesting model structural deficiency at this site as will be discussed later. We therefore did not include ET or VWC from Smith Lake 2 when evaluating the optimal and behavioral parameter sets, in order to avoid introducing objective functions that would select for parameter sets that produce reasonably correct answers for incorrect reasons. Behavioral parameter sets were defined as those with < 0.08 mean RMSE of VWC at the three remaining sites, and < 15% MAE of ET at the site with ET.

2.5 Climate projections

We obtained climate data from the NCAR-CCSM4 and GFDL-CM3 global climate models that were dynamically downscaled using the Weather Research and Forecasting (WRF) model for the years 1970-2100 for the 20 x 20 km grid cells containing each site (Bieniek et al., 2016; Lader et al., 2017). In order to ensure that climate data was relevant to the sites modeled here, we conducted a multivariate quantile mapping bias correction to the gap-filled data for each site (Cannon, 2016). Leaf phenology at both birch-dominated sites was modeled using the relationship between snow disappearance date and leaf-on timing described in Marshall et al. (2020). For each year, we calculated average growing season soil moisture and total growing season ET at the presumed rooting depth at each site with the full set of behavioral parameter sets and evaluated how these trajectories differed between parameter sets. We also used the Hilbert-Schmidt independence criterion to ascertain which parameters contributed most to changes in mean growing season soil moisture in the late-21st century (2070-2099) period relative to a historical (1970-1999) period.

Table 2. Parameters used in study. Parameter names indicate variable name used in figures and a description if applicable. The specifier determines whether the parameter was applied to hardwoods (HW) or conifers (Con), and to mineral (M) or organic (O) soil. Case determines whether the parameter was fixed (F) or calibrated (C), based on the sensitivity analysis. Value is the best estimate when fixed, or calibrated value for parameters that are calibrated.

Category	Parameter	Units	Sites	Specifier	Case	Minimum	Value	Maximum	Sources
Plants	clumping		SL2, SL1	Con	F	0.1	0.4	1	Campbell & Norman, 1998
			UP1A, USRpf	HW	F	0.1	0.7	1	
	CriticalLeafWaterPotential (stomatal resistance twice its minimum value)	m	SL2, SL1	Con	F	-236	-174	-112	Dang et al., 1997; Goldstein et al., 1985
			UP1A, USRpf	HW	F	-275	-174	-100	Cable et al., 2014
	CriticalTranspTemp	°C	SL2, SL1	Con	F	-5	0	5	Bonan & Sirois, 1992; Lamhamedi & Bernier, 1994
			UP1A, USRpf	HW	F	-5	0	5	Ranney & Peet, 1994
	DryBiomass	kg/m^2	SL1, SL2	Con	F	0.1	1.7	17	Alexander et al., 2012; Bonan, 1993; Bond-Lamberty et al., 2002.; Melvin et al., 2015; Viereck et al., 1983; John Yarie & Billings, 2002.
			USRpf	HW	F	2.2	2.1	27	Alexander et al., 2012; Bonan, 1993; Melvin et al., 2015; Viereck et al., 1983; Wang et al., 1995; John Yarie & Billings, 2002. Best estimate is allometric.
			UP1A	HW	F	2.2	4.4	27	
	Interception	m/m	SL2, SL1	Con	C	0	1	1	Li et al., 2017; Link et al., 2004
			UP1A, USRpf	HW	C	0	0.76	1	
	K_{St} (influence of solar radiation on stomatal resistance; 0 = no influence)	W/m^2	SL2, SL1	Con	F	0	20.5	100	Bartlett et al., 2003
			UP1A, USRpf	HW	F	0	50	100	Bladon et al., 2006
	K_{vpd} (maximum reduction in stomatal conductance		SL2, SL1	Con	C	0.1	0.14	1	Grossnickle & Blake, 1986

	due to vapor pressure deficit)		UP1A, USRpf	HW	C	0.1	0.45	1	Bladon et al., 2006
	Leaf area index (LAI)	m^2/m^2	SL1, SL2	Con	C	0.5	1.9	8	Alexander et al., 2012; Bonan, 1993; Bond-Lamberty et al., 2002.; Chen et al., 1997; H. Iwata et al., 2011; Serbin et al., 2013
			USRpf		C		1.8		Bonan, 1993; Chen et al., 1997
			UP1A		C	0.5	4.5	5.7	
	Minimum stomatal resistance ($r_{s,min}$)	s/m	SL2, SL1	Con	C	0.04	1.105	1.174	Bartlett et al., 2003; Cable et al., 2014; Dang et al., 1997; Endalamaw et al., 2017; Körner, 1995; Maire et al., 2015; Salmon et al., 2020
			UP1A, USRpf	HW	C	0.04	0.165	0.178	Blanken et al., 1997; Cable et al., 2014; Dang et al., 1997; Endalamaw et al., 2017; Maire et al., 2015; Murray et al., 2020; Salmon et al., 2020
	PlantAlbedo		SL2, SL1	Con	F	0.1	0.3	0.4	Wide range
			UP1A, USRpf	HW	F	0.05	0.3	0.4	Wide range
	PlantHeight	m	SL1, SL2	Con	C	1	8.8	10	Alexander et al., 2012; Bonan, 1993; Bond-Lamberty et al., 2002; Heijmans et al., 2004
			USRpf		C	1	1.5	3.8	Alexander et al., 2012; Bonan, 1993; Bond-Lamberty et al., 2002.
			UP1A		C	3	7.8	9.9	
	r (coefficient for stomatal conductance due to VPD)		SL2, SL1	Con	C	0.1	0.78	1	Wide range
			UP1A, USRpf	HW	C	0.1	0.11	1	Full possible range
	RootingDepth (maximum rooting depth)	m	SL2, SL1	Con	F	0.1	0.2	0.6	Fryer, 2014
			UP1A, USRpf	HW	F	0.1	0.6	1	Safford et al., 1990
	StomatalExponent (empirical exponent		SL2, SL1	Con	F	2	5	5	Cable et al., 2014

	relating stomatal resistance to leaf potential)		UP1A, USRpf	HW	F	2	5	5	Flerchinger, 2017
	TempLower	°C	SL2, SL1	Con	F	-5	0	5	Bonan & Sirois, 1992; Lamhamedi & Bernier, 1994
			UP1A, USRpf	HW	F	-5	0	0	Ranney & Peet, 1994
	TempOpt		SL2, SL1	Con	C	11	16.7	25	Bonan & Sirois, 1992; Lamhamedi & Bernier, 1994
			UP1A, USRpf	HW	C	20	21.3	40	Ranney & Peet, 1994
	TempUpper		SL2, SL1	Con	F	32	40	50	Bonan & Sirois, 1992; Lamhamedi & Bernier, 1994
			UP1A, USRpf	HW	F	40	46	50	Ranney & Peet, 1994
	TotalResistance (leaf and root resistance)	m^3s/ton	SL2, SL1	Con	C	50	59	5000	Flerchinger, 2017
			UP1A, USRpf	HW	C	250	467	750	Flerchinger, 2017 with 50% increase and decrease
Residue	DryWeightOfResidue	kg/ ha	SL2, SL1	Con	F	1000	6000	10000	Wide range
			UP1A, USRpf	HW	F	1000	6000	10000	Wide range
	FractionResidue		All		F	0	0.9	0.9	Wide range
	ResidueAlbedo		All		F	0.15	0.25	0.4	Flerchinger, 2017
	ResidueThickness	cm	SL2, SL1	Con	F	0	5	20	Wide range
			UP1A, USRpf	HW	F	1	5	20	Wide range
Site	ponding	cm	All		C	2.5	1.2	10	Wide range
	PrecipThreshold (precipitation falls as snow below this temperature)	°C	All		F	-0.4	1	2.4	Jennings et al., 2018
	roughness (of residue or soil surface)	cm	All		F	0.1	1	10	Campbell & Norman, 1998

Soils	AlbedoDrySoil		All		F	0.1	0.25	0.4	Flerchinger, 2017
	AlbedoExponent (Exponent for albedo of moist soil)		All		F	0.1	0.1	3.5	Flerchinger, 2017
	bulkdensity 1 (ρb 1)	kg/m^3	UP1A	M	C	700	913	1720	NCSS, 2020
			USRpf, SL2, SL1	O	C	10	262	300	Liu & Lennartz, 2019
	bulkdensity 2 (ρb 2)		All	M	C	700	1158	1720	NCSS, 2020
	bulkdensity 3 (ρb 3)		All	M	C	700	1223	1720	NCSS, 2020
	ksat 1 (saturated hydraulic conductivity)	cm/hr	UP1A	M	C	0.027	234	270	Blain & Milly, 1991; Chappell et al., 1998; Grayson et al., 1992; NCSS; 2020
			USRpf, SL2, SL1	O	C	0.0017	443	1148	Liu & Lennartz, 2019
	ksat 2		All	M	C	0.027	181	270	Blain & Milly, 1991; Chappell et al., 1998; Grayson et al., 1992; NCSS, 2020
	ksat 3		All	M	C	0.027	141	270	Blain & Milly, 1991; Chappell et al., 1998; Grayson et al., 1992; NCSS, 2020
	lowerBC (soil temperature at lower boundary)	°C	USRpf		F	0	2.4	5	Soil temperature observations
			SL2		F	-5.1	-1.1	2.9	Soil temperature observations
			SL1		F	-4.4	-0.4	3.6	Soil temperature observations
			UP1A		F	0	0.5	5	Soil temperature observations
	poreconn 1 (τ 1; van Genuchten pore connectivity)		USRpf, SL2, SL1	O	C	-5.22	-1.66	1.06	Liu & Lennartz, 2019
	residual volumetric water content 1 (θres 1)		UP1A	M	C	0.017	0.021	0.14	NCSS, 2020
			USRpf, SL2, SL1	O	C	0.004	0.149	0.2	Liu & Lennartz, 2019

	θres 2		All	M	C	0.017	0.071	0.14	NCSS, 2020
	θres 3		All	M	C	0.017	0.088	0.14	NCSS, 2020
	θsat 1		UP1A	M	C	0.34	0.566	0.59	NCSS, 2020
			USRpf, SL2, SL1	O	C	0.62	0.625	0.99	Liu & Lennartz, 2019
	θsat 2		All	M	C	0.34	0.546	0.59	NCSS, 2020
	θsat 3		All	M	C	0.34	0.454	0.59	NCSS, 2020
	van Genuchten alpha (vG α 1)	m^{-1}	UP1A	M	C	0.65	4.44	5.1	NCSS, 2020
			USRpf, SL2, SL1	O	C	1	30.2	45	Liu & Lennartz, 2019; limited upper range because model failed above ~45
	vgAlpha_2 (van Genuchten alpha) (vG α 2)		All	M	C	0.65	2.3	5.1	NCSS, 2020
	vgAlpha_3 (van Genuchten alpha) (vG α 3)		All	M	C	0.65	4.77	5.1	NCSS, 2020
	vgn_1 (van Genuchten n) (vG n 1)		USRpf, SL2, SL1	O	C	1.29	1.54	1.6	Dettmann et al., 2014; Zhang et al., 2010

3 Results

3.1 Parameter sensitivity

At the permafrost-underlain Smith Lake site, growing season θ_{VWC} at the assumed maximum rooting depth (20 cm) was most sensitive to soil hydraulic parameters in the depth at which soil moisture was assessed (layer 1), as well as parameters that control plant water use, including minimum stomatal resistance ($r_{s,min}$), LAI, the Jarvis-Stewart r parameter that controls the influence of vapor pressure deficit on stomatal resistance, and total resistance in leaves and roots (Figure 3). Growing season θ_{VWC} was also sensitive to K_{sat} in the second layer and van Genuchten α in the third layer, as well as maximum canopy interception depth per LAI and aspect. Results at the US-Rpf site were similar. The top four parameters with the largest influence on growing season θ_{VWC} at 60 cm were soil hydraulic parameters in the layer at which soil moisture was evaluated; soil hydraulic parameters for the other layers, particularly α, k_{sat}, and θ_{res} were also important in the sub- and superjacent layers. As at Smith Lake, $r_{s,min}$ and r were significant. Notably, peak LAI at this site was not statistically significant, while a few additional controls on plant hydraulics were: optimum transpiration temperature, plant height, and K_{vpd} were all statistically significant. Moreover, slope and maximum ponding depth, in addition to aspect, were significant at this site.

To assess the sign of the parameter effects, we compared parameter distributions for the wettest and driest simulations at each site (Figure 4). Distributions that are very dissimilar between the wettest and driest simulations indicate that a parameter has a strong and consistent effect, while those with large overlap indicate either weaker effects or that parameter interactions are more important than the parameter value itself. Many of these are to be expected based on a priori knowledge of the physics represented in the SHAW model: for example, high LAI, low $r_{s,\,min}$, and south-facing aspects reliably result in drier soils. Similarly, in the layer at which growing season θ_{VWC} was evaluated at each site, low θ_{res}, low θ_{sat}, and higher α tend to result in drier θ_{VWC}. Less obvious are the contrasting effects of soil hydraulic parameters in sub- and superjacent layers: for example, at the US-Rpf site, high θ_{res} in the third layer tends to yield drier θ_{VWC} in the second layer. While this is also a natural consequence of the physics represented in the model, it may be less obvious to modelers conducting manual parameterizations. Finally, some parameters, such as plant height and maximum interception, have a statistically significant effect on growing season θ_{VWC} but limited discernable difference in their distributions between the driest and wettest 1% of cases. This may suggest that the HSIC metric is identifying parameters with a relatively small effect size, or that there are complex parameter interactions that minimize the relationship between an individual parameter and θ_{VWC}.

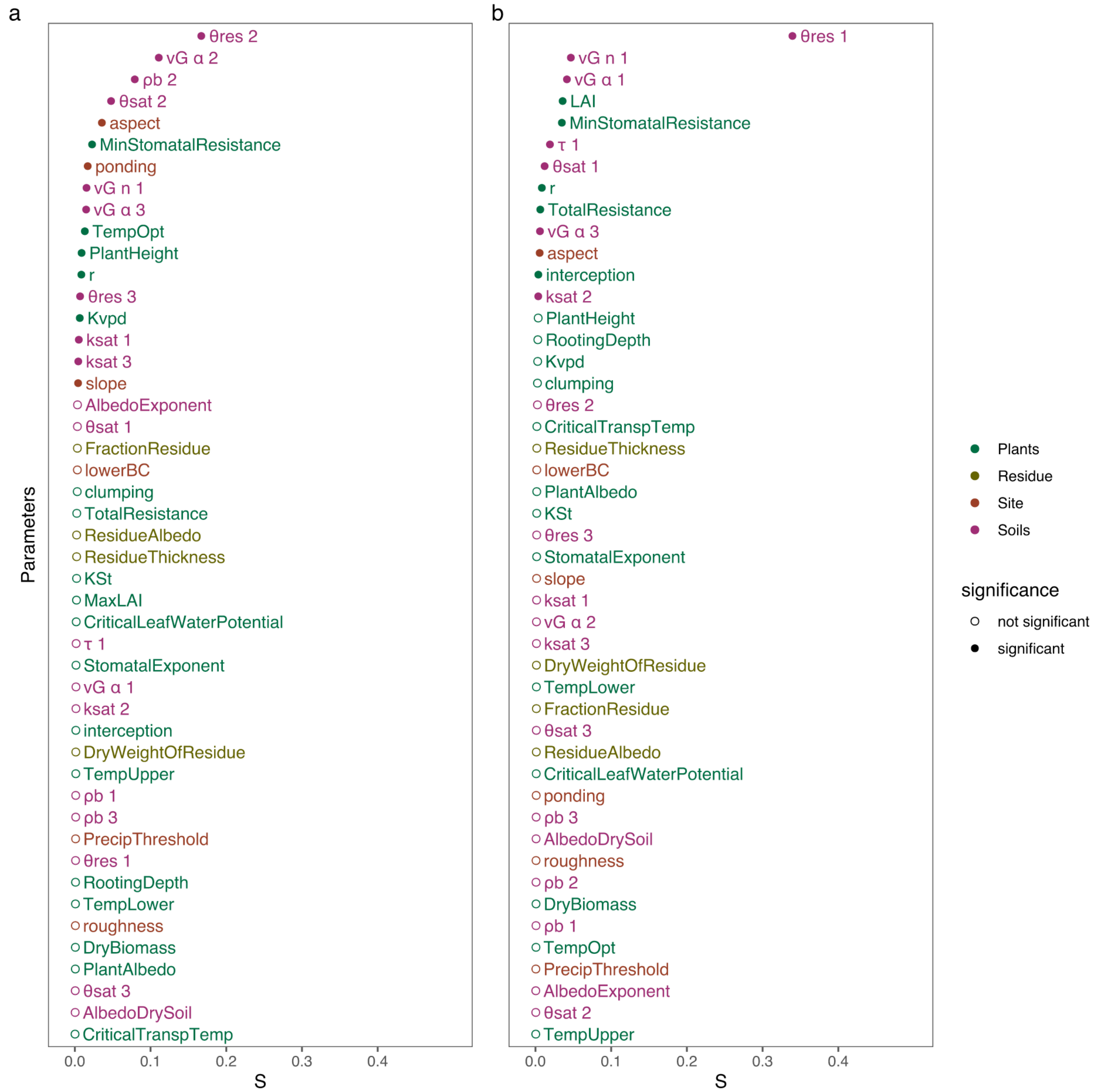

Figure 3. Results of sensitivity analysis at (a) US-Rpf and (b) Smith Lake 2. Significance threshold was $p < 0.034$ at US-Rpf and $p < 0.016$ at Smith Lake 2. S is the Hilbert-Schmidt Independence Criterion.

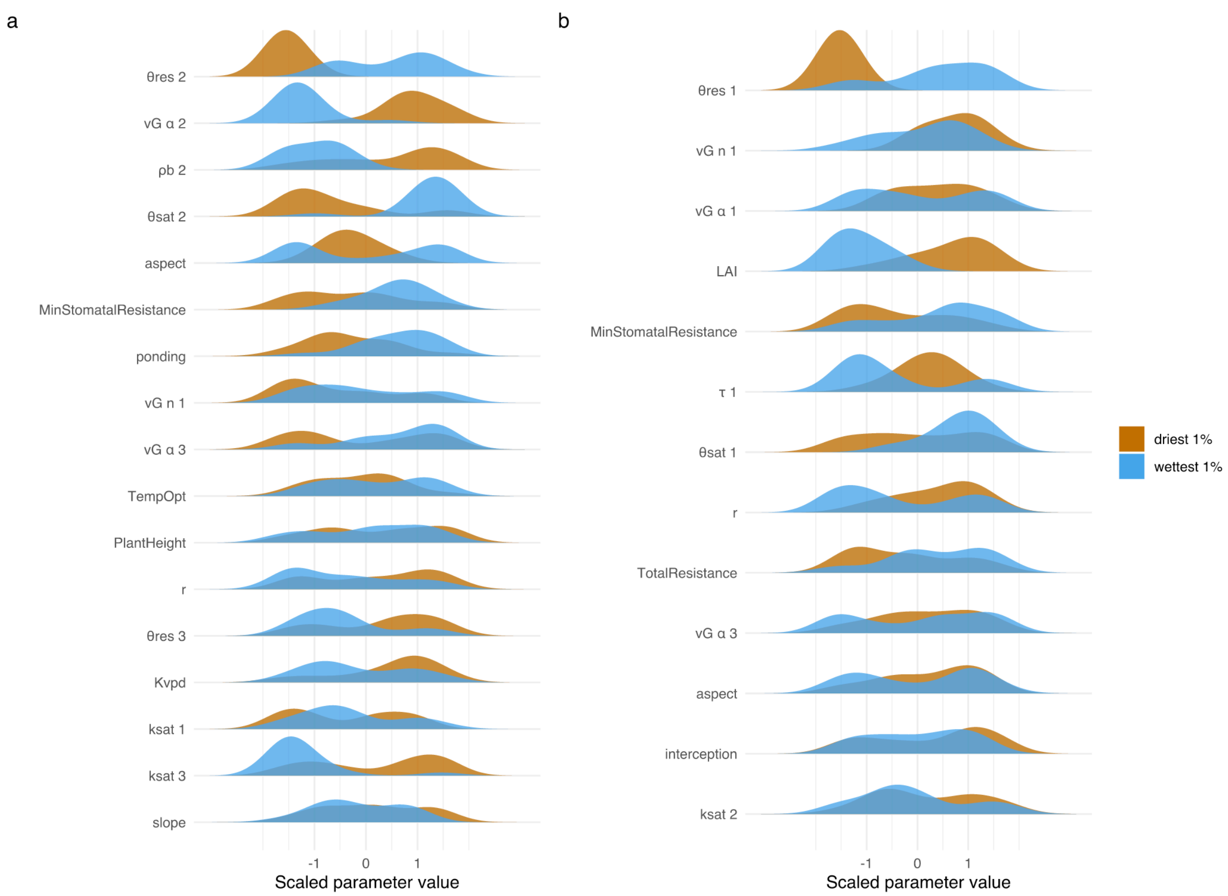

Figure 4. Distribution of the statistically significant parameter values for the driest and wettest 1% of runs at (a) US-Rpf and (b) Smith Lake 2. Parameter abbreviations are detailed in Table 2.

3.2 GLUE results

In the GLUE analysis, 40% of 22,664 parameter sets completed the model runs at all four sites, with some differences between sites: 99.8% finished at UP1A; 77.0% finished at Smith Lake 2; 69.5% finished at Smith Lake 1; and 61.2% finished at US-Rpf. Runs that do not complete are likely due to unrealistic parameter combinations that cause numerical instabilities in the finite difference solutions employed in the SHAW model. The minimum θ_{VWC} RMSE between sites suggests some discrepancy between performance at each site: at Smith Lake 1 and 2, the minimum RMSEs were 0.087 and 0.111, respectively, while these values were 0.026 and 0.030 at UP1A and US-Rpf. Minimum MAE of ET was 3.3% and 9.6% at Smith Lake 2 and US Rpf, respectively. After Smith Lake 2 results were discarded due to poor simulation of soil moisture, 45% of parameter sets completed the model run at the three remaining sites. Correlations between objective functions suggested some tradeoffs and synergies: for example, θ_{VWC} RMSE at US-Rpf was positively correlated with that at Smith Lake 1 (Pearson's $r = 0.5$), while

RMSE of VWC at UP1A was negatively correlated with θ_{VWC} RMSE at both US-Rpf and Smith Lake 1, indicating that there are tradeoffs in parameter selection between UP1A and the other two sites. MAE of ET was positively correlated with θ_{VWC} RMSE at US-Rpf ($r = 0.3$), implying that parameter sets that modeled ET well tended to also model θ_{VWC} well.

The criteria for behavioral parameter sets, with MAE ET at US-Rpf less than 15% and mean θ_{VWC} RMSE across three sites < 0.08, resulted in 27 parameter sets. The distributions of behavioral parameter sets suggested that some, but not all of the parameters were better constrained post calibration (Figure 5), as indicated by less variable (e.g. LAI at UP1A) as opposed to similar (e.g.: θ_{sat} 2M) posterior parameter distributions. Note that in some cases, a uniform prior distribution was not used, due to our restrictions on the changes in some soil hydraulic parameters with depth. In behavioral parameter sets, bulk density of the organic layer tended to be high relative to the prior distribution. LAI was at the low end of the distribution at the US-Rpf site, and higher at the UP1A site. $r_{s,min}$ was generally higher in the posterior than prior distribution. The van Genuchten pore connectivity term, τ, in the organic layer was generally in the higher range of the prior distribution, and van Genuchten α was relatively high in the organic layer, but low in the first and second mineral soil layers. Parameter values based on individual sites or objective functions were quite different from each other in many cases, illustrating the importance of calibration on multiple sites and hydrologic variables when possible.

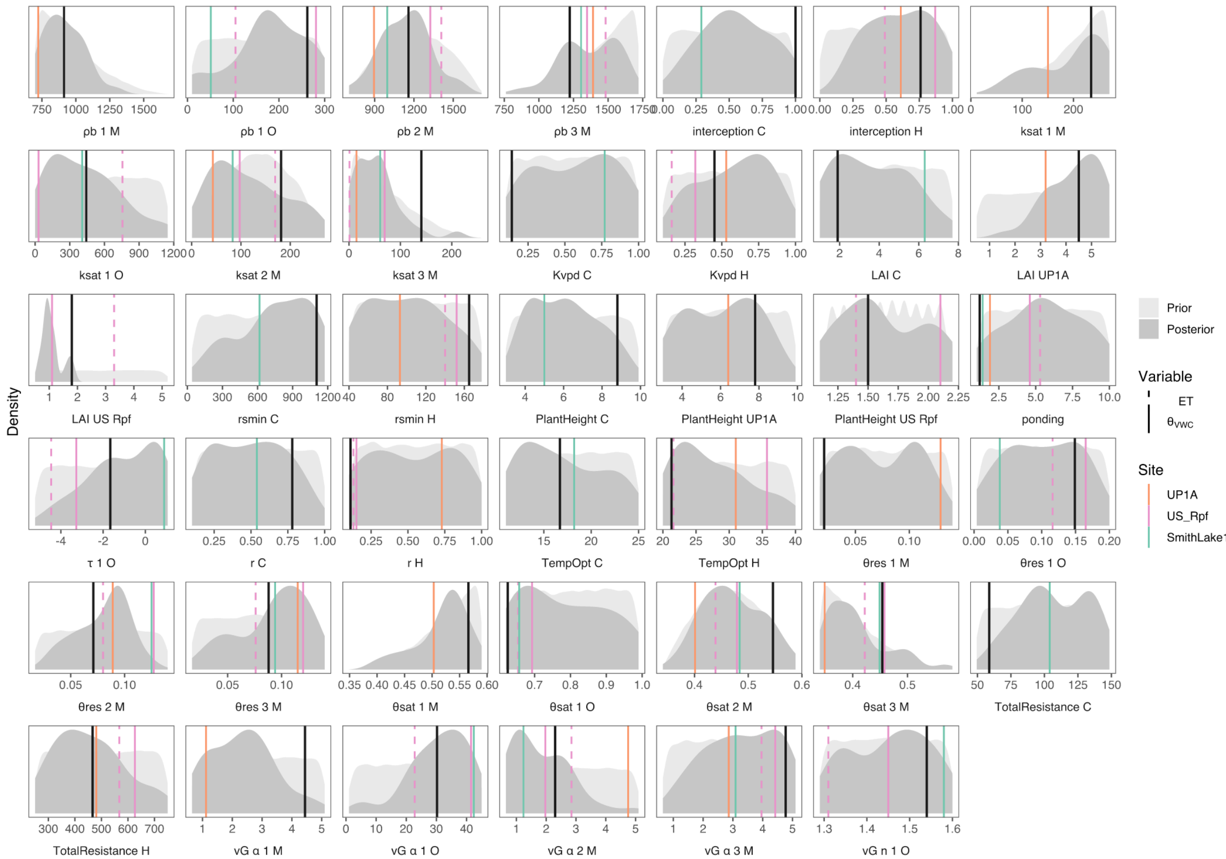

Figure 5. Distribution of behavioral parameter sets. Vertical lines for each site (colors) and variable used in the objective function (line type) indicate the parameter values in the optimal parameter set for each site and variable. The black vertical lines indicate the best overall parameter. Parameter abbreviations are detailed in Table 2.

The optimal parameter set based on multiple objective functions resulted in θ_{VWC} RMSE of 0.10 at Smith Lake 1, 0.05 at UP1A, and 0.08 at US-Rpf, with MAE ET at US-Rpf equal to 9.0%. This parameter set had considerably higher interception per LAI, K_{vpd} in conifers, and LAI in conifers and at UP1A than the best prior estimates. The best estimate of $r_{s,min}$ was slightly higher in conifers and lower in hardwoods than the best prior estimate. Optimum temperatures for transpiration were quite close to the best prior estimate. The best estimated maximum ponding depth was at the very high end of the potential range. K_{sat} was much higher in mineral layers and lower in the organic layer than the best prior estimate; this may reflect in part the fact that values for mineral layers were obtained directly from a lab-based database, while values for organic layers were obtained from literature with values presented over many orders of magnitude. τ, which is often set to 0.5 in mineral soils but may be much lower in organic horizons (Dettmann et al., 2014), was much higher than the best estimate for organic soils, and close to the typical value in mineral soils. van Genuchten α was considerably larger in both the mineral and organic layers than best prior estimates.

3.3 Reproduction of soil moisture and ET

SHAW generally reproduced temporal soil moisture patterns well, but the multi-site solution represented tradeoffs for individual sites (Figure 6). For example, the parameter set that minimized θ_{VWC} RMSE at US Rpf resulted in θ_{VWC} that was consistently too high at UP1A, and too low at Smith Lake 1. Parameter sets that performed well at three sites performed extremely poorly at Smith Lake 2, and in many cases model convergence issues prevented the runs from completing at that site. In addition to the overall poor performance at Smith Lake 2, this reinforces the finding that model structural deficiency likely limits model performance at this site. The multisite compromise tended to be somewhat too dry in the summers at Smith Lake 1 and too wet in the winters at US-Rpf, but captured soil moisture dynamics at UP1A very well.

Comparisons of modeled and observed ET at US-Rpf indicate that the behavioral parameter sets generally contained observed summer ET and consistently underestimated winter ET (Figure 7). The best parameter set and the set based on minimizing MAE ET tended to overestimate summer ET. In contrast, the set that was selected to minimize the θ_{VWC} RMSE at US-Rpf tended to underestimate ET. Model performance generally declined slightly from the calibration to validation period with respect to θ_{VWC} RMSE. In the multisite compromise, θ_{VWC} RMSE increased from 0.112 to 0.123 at Smith Lake 1 (+0.011), from 0.072 to 0.079 at UP1A (+ 0.007), and from 0.054 to 0.072 at US-Rpf (+0.017). The MAE of ET actually decreased from the calibration to validation period, from 18% to 14% (-4%).

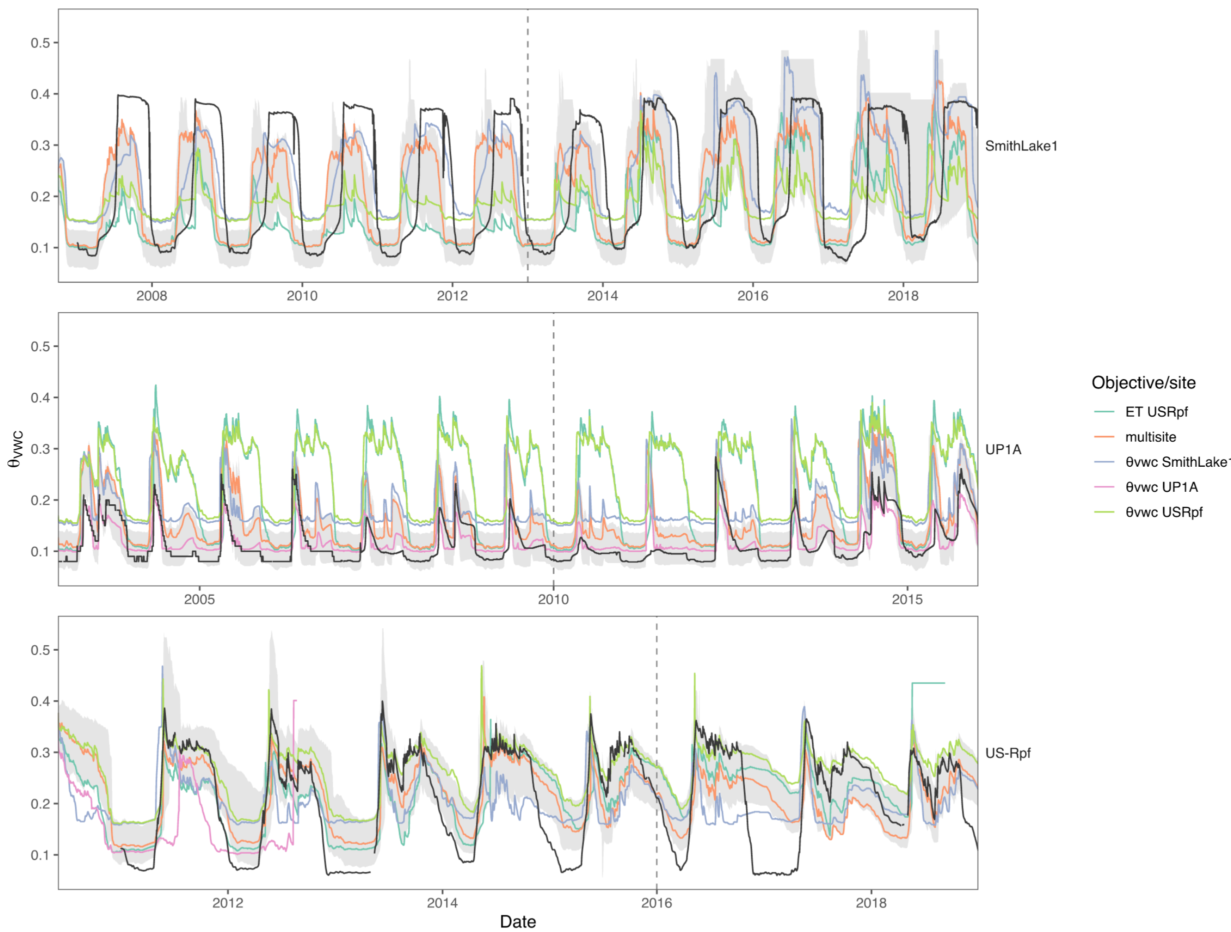

Figure 6. Observed and modeled soil moisture for each site. The black line represents observations at approximate rooting depth at each site, and the colored lines represent multiple selected model parameters based on individual objective functions and a multisite compromise. Gray error bars indicate the range of values simulated by the behavioral parameter sets. Vertical dashed line indicates transition from calibration to validation period.

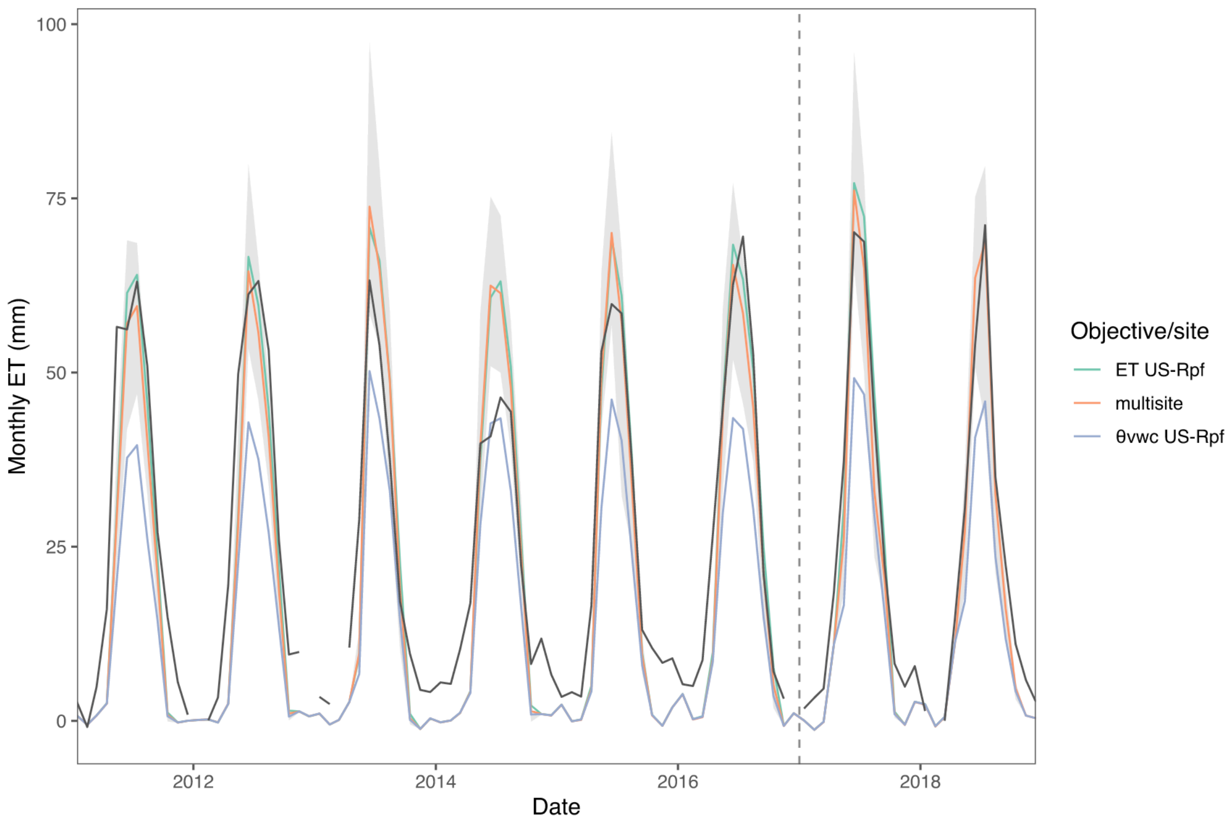

Figure 7. Observed and modeled monthly ET at US-Rpf, the only site where ET was available. Gray shaded area represents the range of all behavioral parameter sets; black line represents observations, and colored lines represent selected parameter sets as indicated in the legend. Vertical dashed line indicates transition from calibration to validation period.

3.4 Climate projections and sensitivity

Climate projections in bias-corrected, dynamically downscaled NCAR-CCSM4 and GFDL-CM3 indicate increases from 1970-2000 to 2070-2100 in mean annual temperature ranging between sites from 10.3-12.5 °C in GFDL-CM3 and 6.4-7.7 °C in NCAR-CCSM4 (Figure 8). The range of changes in projected precipitation is much greater between GCMs and sites, with projected changes in GFDL-CM3 much greater than those in NCAR-CCSM4. At US-Rpf, projected increase in precipitation was 13.1-36.0%, depending on GCM; projected increase in precipitation was 68-190% at UP1A and 72-396% at Smith Lake 1. This exaggerated large increase in precipitation in GFDL-CM3 at Smith Lake 1 is due in part to the bias-correction: the uncorrected, downscaled data in GFDL-CM3 has 510 mm of precipitation at Smith Lake 1 in 1970-2000, but the bias-corrected data has only 139 mm; in the 2070-2100 period, the downscaled data has 940 mm while the bias-corrected results has 690 mm. The absolute differences are reasonably comparable between the bias-corrected and downscaled data, but the percent differences increase dramatically due to the smaller denominator in the bias-corrected data.

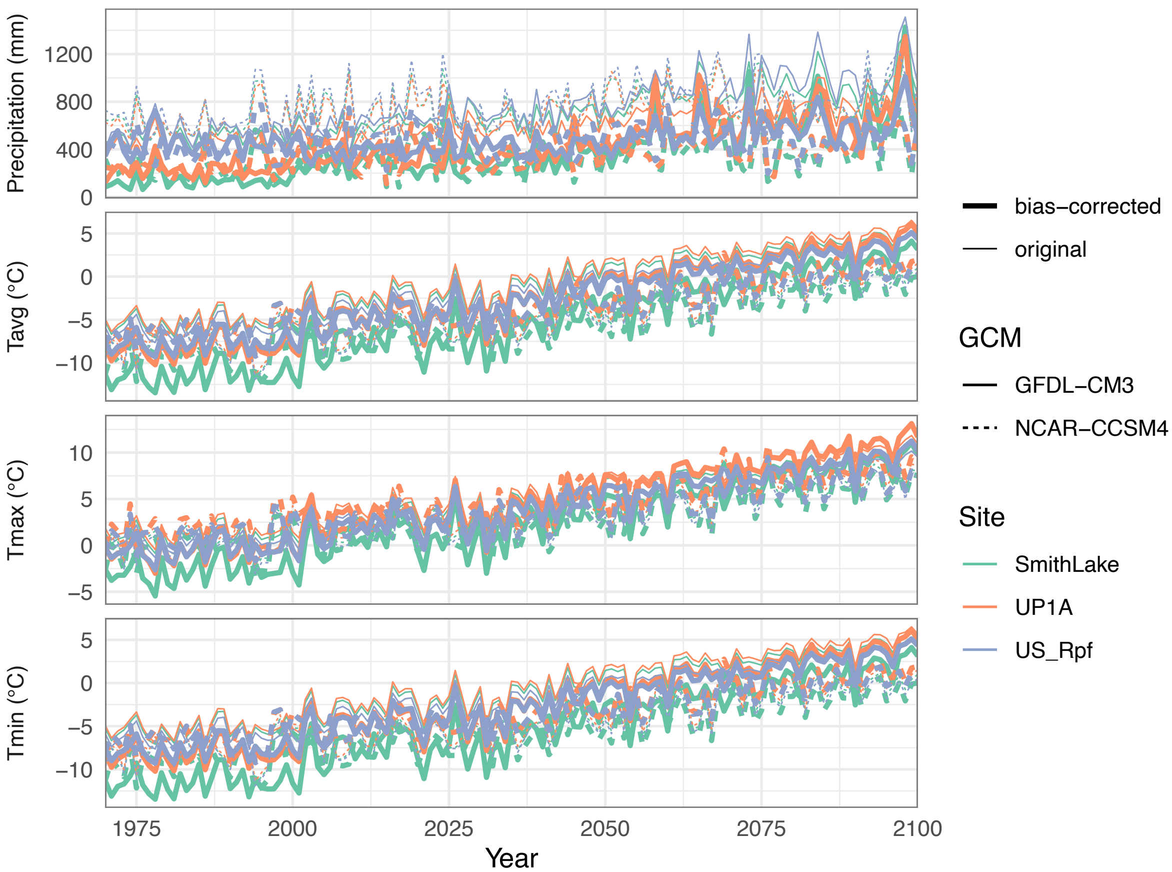

Figure 8. Projections of future climate variables with two GCMs, summarized annually. Thicker lines indicate bias-corrected data, while thin lines show the WRF-downscaled data.

Choice of parameter set and GCM had comparable effects on trends in growing season θ_{VWC} to the total effect of climate change, though these differences varied considerably between sites (Table 3; Figure 9). At Smith Lake 1, growing season θ_{VWC} was projected to change by an average of +0.067 ± 0.211 cm^3/cm^3 in GFDL-CM3 and -0.095 ± 0.157 cm^3/cm^3 in NCAR-CCSM4. In both GCMs, the high standard deviation relative to the mean change suggests that the variability due to parameter selection is greater than the projected impacts of climate change, and that even the sign of the projected change depends on GCM choice and parameter selection. Moreover, the difference between mean results for each GCM (0.162 cm^3/cm^3) is greater than the mean projected impacts of climate change in either GCM, and is of a similar magnitude to the uncertainty due to parameter set selection. At UP1A, the mean projected change in growing season θ_{VWC} was greater than the standard deviation across parameter sets in both GCMs, suggesting that the impacts of climate change in this case were greater than those of parameter selection; notably, the mean impacts of climate change in NCAR-CCSM4 were almost zero. GCM choice was also important in this case, with considerable wetting in GFDL-CM3 and almost zero mean change in NCAR-CCSM4. At US-Rpf, the mean effect of climate change was greater than parameter set variability in GFDL-CM3, but not in NCAR-CCSM4. In US-Rpf as in UP1A, the mean changes in growing season θ_{VWC} were close to zero with NCAR-CCSM4 forcing but showed considerable wetting across most parameter sets in GFDL-CM3.

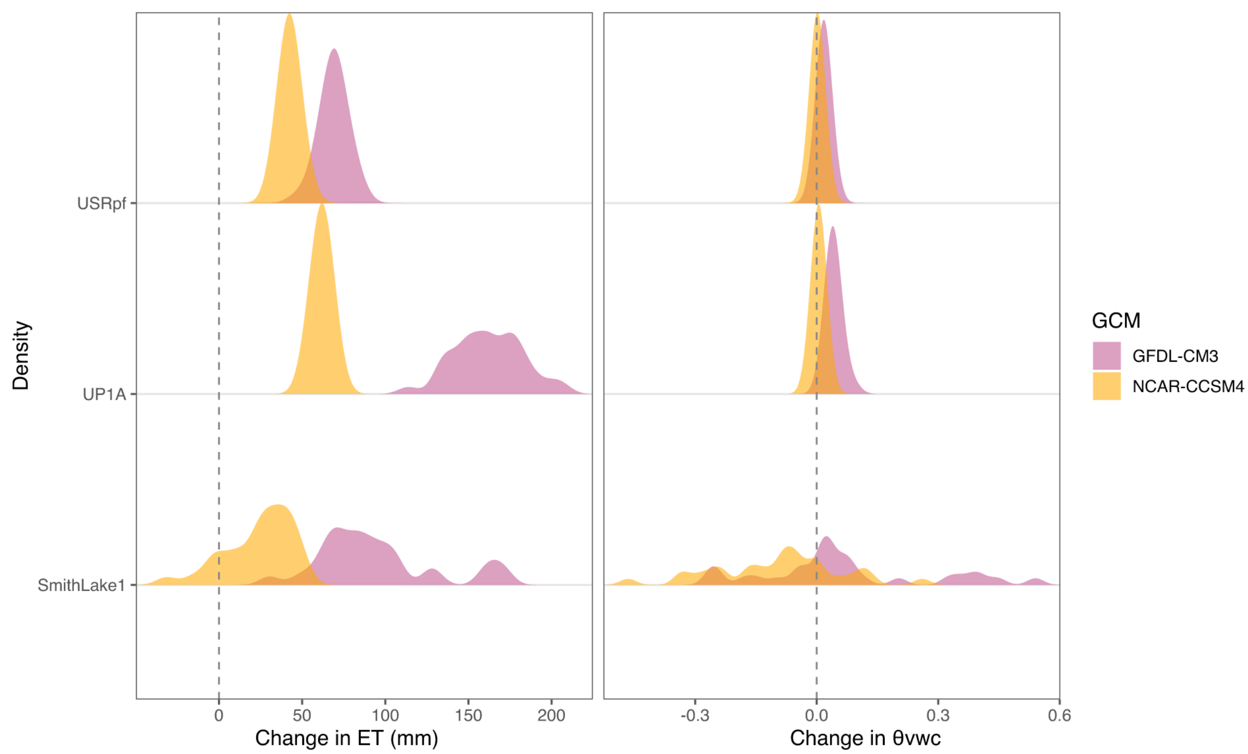

Figure 9. Percent change from 1970-2000 to 2070-2100 in growing season ET (left) and mean θ_{VWC} at approximate rooting depth (right) for 35 behavioral parameter sets at each site in two GCMs.

Table 3. Mean and standard deviations of projected changes in growing season soil moisture and ET between sites and GCMs.

GCM	**Site**	**Change in θ_{VWC} (%)**	**Change in ET (%)**
GFDL-CM3	SmithLake1	0.067 ± 0.211	94 ± 36
NCAR-CCSM4		-0.095 ± 0.157	24 ± 20

GFDL-CM3	UP1A	0.042 ± 0.014	162 ± 21
NCAR-CCSM4		0.005 ± 0.003	62 ± 5
GFDL-CM3	USRpf	0.018 ± 0.006	69 ± 8
NCAR-CCSM4		0.002 ± 0.002	42 ± 5

Changes in ET were predominantly positive, and the relative effect of parameter sets, GCM, and climate change varied between sites. At Smith Lake 1, the projected change in ET was greater than the standard deviation across parameter sets for both GCMs, though the mean difference between GCMs (70 percentage points) was greater than the average projected change in ET by NCAR-CCSM4. At UP1A, change in ET was less dependent on choice of parameter set, but there was a difference of 100 percentage points in the projected mean change between the two GCMs. At US-Rpf, results were more consistent between GCMs and parameter sets: the mean difference in ET increase between the two GCMs was only 27 percentage points, and the coefficient of variation across parameter sets was approximately 9 for both GCMs.

Some parameters contributed more to future wetting or drying trends than others, though relatively few have a statistically significant effect on wetting or drying trends (Figure 10). The only parameter with a statistically significant effect on change in future θ_{VWC} was maximum ponding depth, and it had a statistically significant effect only at USRpf. Higher maximum ponding depth tended to result in reduced θ_{VWC} in the simulations forced with NCAR-CCSM4 (Figure 11). At UP1A, higher θ_{sat} in the first and second layers, and a higher *r* in the Jarvis-Stewart stomatal conductance functions all had a statistically significant effect on changes in ET, and higher values of these parameters tended to result in higher increases in ET in the simulations forced with GFDL-CM3.

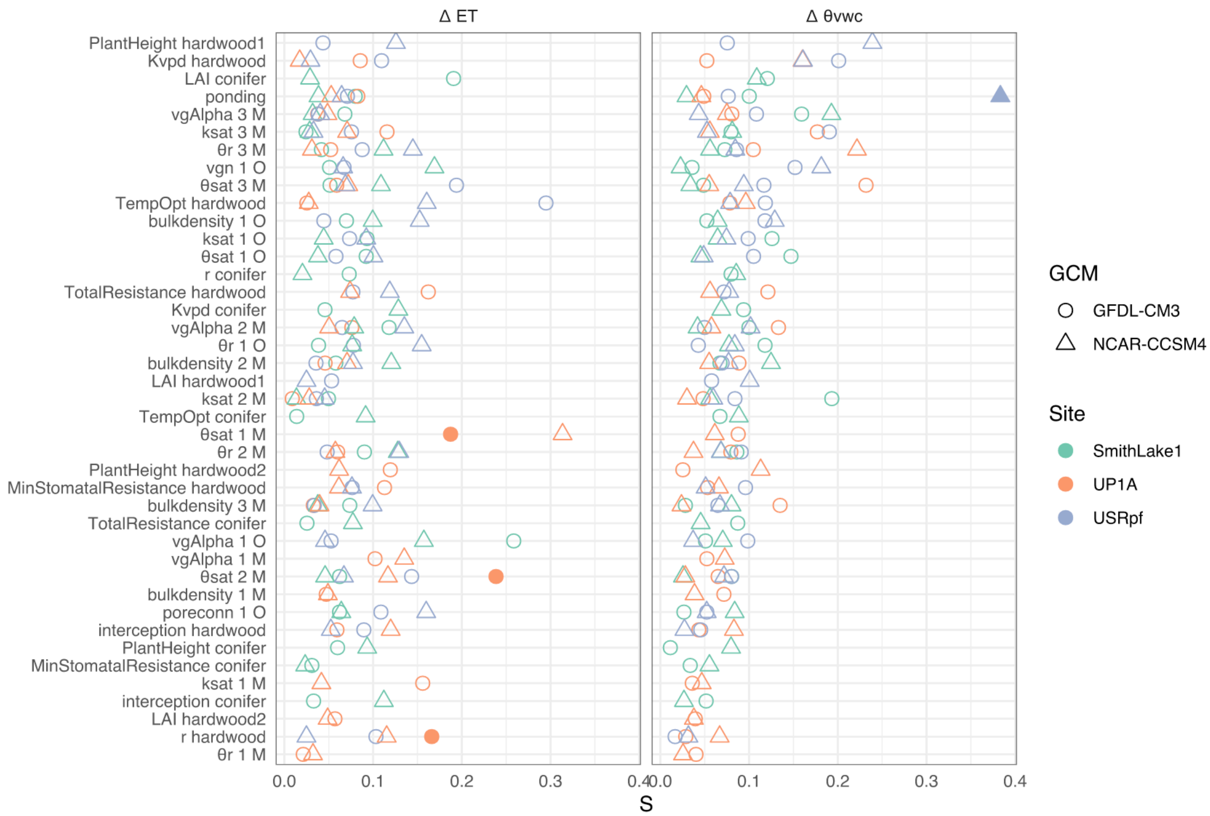

Figure 10. HSIC results showing parameters at each site to which change in ET and change in growing season soil moisture are sensitive. Parameters are ordered based on their mean S across sites and GCMs. The filled points were statistically significant, with p-values indicating that the false discovery rate was less than 0.1 for each site. O = organic; M = mineral and numbers 1-3 indicate soil layer; see Table S1 for additional parameter descriptions.

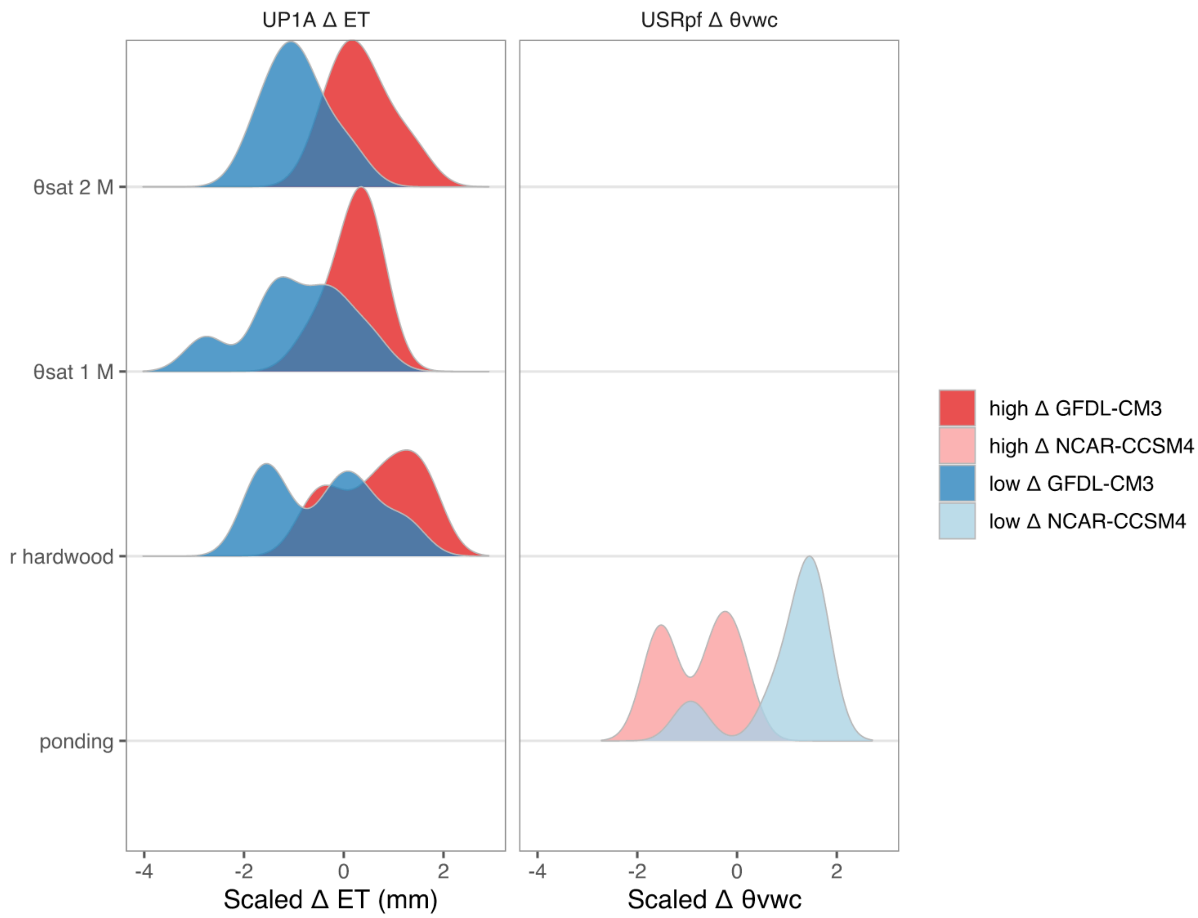

Figure 11. Distribution of scaled parameter values that contribute to the results with the largest and smallest 20% of changes in VWC or ET at each site. Only statistically significant parameters are shown; some site/variable combinations had no significant parameters.

4 Discussion

4.1 Sensitivity analysis

At both sites, the most influential inputs were the van Genuchten hydraulic parameters in the soil layer in which soil moisture was evaluated. Soil hydraulic parameters in subjacent layers were also quite sensitive in some cases, though they often had the opposite direction of effect: for example, higher θ_{VWC} in the target layer was associated with higher α in that layer, but lower α in the subjacent layer. This is consistent with the model physics, but may not be immediately obvious during manual calibration. It is also an example of a parameter interaction that should be taken into consideration when interpreting and determining hydrologic model parameters. The sensitivity results also depend to some extent on the width of the prior distributions, which were determined by a detailed literature review. The results should therefore be interpreted with the view that the prior distributions are necessarily somewhat subjective, depending on available literature and modeler interpretation of that literature. Nevertheless, the results of the sensitivity analysis suggest that soil hydraulic parameters throughout the soil profile should be carefully considered in ecohydrological model calibrations.

4.2 Parameter estimation and uncertainty

SHAW was able to simulate soil moisture dynamics reasonably well across multiple sites over 8-13 years. Parameter sets were identified to minimize error at individual sites, but a multisite, multiobjective compromise parameter set also provided acceptable performance. The decline in performance of the compromise parameter set relative to those that performed best at individual sites highlights the risks of overfitting the model to an individual site or objective. Previous comparable modeling studies in boreal regions have found mean error of soil moisture in the rooting zone equal to 0.02, which is lower than the error we generally found when multiple sites were included (Launiainen et al., 2019). Several other soil moisture modeling studies in boreal regions note the difficulty of modeling soil moisture, relative to soil temperature, and provide figures illustrating observed and modeled soil moisture, but lack fit statistics for comparison (Houle et al., 2012; Jones et al., 2014). The relatively poor model performance at Smith Lake 2, particularly relative to the other sites, suggests a model structural deficiency. Most likely, this is due to the low slope and topographic position and potential for high net lateral flow at this site given the one dimensional nature of the SHAW model. Recent improvements in SHAW have allowed for the inclusion of subsurface lateral flow, which could facilitate the use of SHAW in lowland regions.

The results of our GLUE uncertainty analysis indicate that most parameters were not very well constrained relative to the prior distributions, though the parameters that had high sensitivity and were only used at one site (e.g., LAI at each of the hardwood sites) tended to be relatively well constrained by the calibration. This suggests that differences between sites limit parameter identifiability within our modeling context. An alternative to the approach presented here would be to calibrate SHAW against fully spatially distributed data products, whether remotely sensed or interpolated (Zwieback et al., 2019). While this would provide more explicit spatial variability, it also introduces additional errors in the calibration data, which run the risk of contributing disinformative data (Beven & Westerberg, 2011). Future improvements to our method could leverage data from more sites and include more stratification of soils by texture and organic layer class (i.e., live moss vs dead moss). However, this is limited by the availability of sites with high quality climate data inputs and validation data. For instance, in the AmeriFlux site network, which provided important data for this study, there are about twice as many sites per km^2 in the contiguous United States as in Alaska (25 sites per million km^2 in Alaska, and 47 sites per million km^2 in CONUS). In interior Alaska, upland sites with these data characteristics are particularly rare and are more appropriate for the SHAW model than lowland sites with large expected net subsurface lateral flows (Govind et al., 2011).

Another finding of note was that the parameter set that minimized θ_{VWC} RMSE at US-Rpf tended to underestimate ET at the same site. This may suggest tradeoffs between soil hydraulic and plant hydraulic parameter accuracy. For instance, this parameter set had low LAI and high $r_{s,min}$, which may have reduced plant water use and controlled soil moisture in rooting depth via relatively high van Genuchten α in the adjoining layers. While the wide range of parameter values in the literature makes it difficult to constrain these parameters, multi-objective model calibration can reduce equifinality to some extent, in alignment with previous findings (Efstratiadis & Koutsoyiannis, 2010).

4.3 Climate projection uncertainty

In this study, parameter uncertainty and GCM choice contributed about as much to future soil moisture and ET uncertainty as the total effect of changing climate in the less sensitive GCM, NCAR-CCSM4. This finding reinforces the importance of assessing and reporting sensitivity and uncertainty in environmental simulation models (Saltelli et al., 2019), and, in addition to model structure, may explain some of the spread in projected future soil moisture across multiple hydrologic models when parameter uncertainty is not accounted for (Andresen, 2020). Our finding that parameter uncertainty is quite important contrasts somewhat with previous studies (Dobler et al., 2012; Feng & Beighley, 2020), though these have focused primarily on discharge in temperate regions. This could be because the effects of climate change on soil moisture and ET in boreal Alaska are relatively small compared to projected changes in discharge in temperate regions, or it could suggest that our criteria for behavioral parameter sets are looser than previous studies, though this is difficult to directly assess. These results highlight challenges related to subjectivity in choices of "behavioral" parameter sets, GCMs used as input data, and the climate scenario considered. This inherent subjectivity may be impossible to eradicate from the practice of modeling, but should be recognized and explicitly considered when interpreting model results.

Finally, our results demonstrate the effects of individual parameters on projected changes in soil moisture and ET. In general, soil moisture in SHAW and similar models can be controlled via soil hydraulic and plant hydraulic parameters, with equifinality in the balance between the two. The parameters that have a statistically significant effect on change in ET and soil moisture vary between sites and objective, but include θ_{sat}, ponding, and the Jarvis-Stewart *r* parameter, which controls the shape of the stomatal conductance response to vapor pressure deficit, with high values resulting in more sensitivity of stomatal conductance to vapor pressure deficit. While the statistical significance of these parameters varies between the GCMs used for forcing and sites, the effect directions are consistent with expectations. For example, high θ_{sat} in the first and second soil layers tended to increase ET. This could be due to the fact that higher water holding capacity can exceed evaporative demand in historical conditions but not in future conditions, leading to large increases in ET. Similarly, higher values of *r* tended to result in greater increases in ET, which is to be expected in energy-limited environments, where ET may be primarily sensitive to vapor pressure deficit. While previous studies have quantified the uncertainty in future climate projections that can result from equifinality (Mendoza et al., 2016), the effect direction of particular parameter choices has not, to our knowledge, been previously assessed quantitatively. Even in contexts in which a full uncertainty analysis is not feasible, we suggest that modelers should explicitly consider and discuss their parameter value selection relative to known ranges of values, and the potential effects of these parameter selections on projected climate change impacts in a given model.

5 Conclusions

In this study, we conducted a global sensitivity analysis of a process-based hydrologic model at two contrasting boreal sites, providing a screening and ranking of sensitive parameters. Soil hydraulic and plant hydraulic parameters were most sensitive at both sites. We calibrated these sensitive parameters in a GLUE parameter calibration and uncertainty analysis against soil moisture and ET, and identified parameters that were most successful in reasonably reproducing VWC and ET across multiple sites. Critically, we note that the parameter sets identified here should be considered not as an absolute truth, but as a useful set of parameters for modeling in upland boreal forests. Finally, we compared the effect of parameter and GCM selection on changes in soil moisture and ET, finding that these selections can influence the magnitude of projected changes about as much as the total impact of projected climate change, and in some cases, can even influence the sign of projected changes. In a novel contribution, we also identified the parameters to which projected changes in hydrology were most sensitive and the direction of effect of these parameters. While previous studies have assessed the importance of equifinality for climate change impacts assessments, this assessment of the most important parameters and direction of their effects can provide guidance to modellers and consumers of modeling studies who want to understand how specific parameter selections affect estimates of climate change impacts on hydrologic states and fluxes in boreal regions.

Acknowledgments, Samples, and Data

This research was funded by NSF Grant #1737413. We are extremely grateful for the decades of data collection efforts at the Bonanza Creek LTER, US-Rpf and US-Uaf Ameriflux sites, and Smith Lake sites via the Geophysical Institute at the University of Alaska Fairbanks. Bertrand Iooss provided valuable guidance on sensitivity analysis methods. We respectfully acknowledge that data used in this research was gathered on the ancestral and unceded traditional territories of the lower Tanana Dene Peoples and the Dena'ina Peoples.

Data used to develop model inputs are available as cited throughout the methods section. SHAW model inputs and outputs used in this manuscript are published as: Marshall et al. (2021) SHAW model inputs and outputs in boreal Alaska, Hydroshare, https://www.hydroshare.org/resource/5a355d67357a4b8591def61602fe276b/.

References

Alexander, H. D., Mack, M. C., Goetz, S., Beck, P. S. A., & Belshe, E. F. (2012). Implications of increased deciduous cover on stand structure and aboveground carbon pools of Alaskan boreal forests. *Ecosphere*, *3*(5), art45. https://doi.org/10.1890/ES11-00364.1

Anderson, E. A. (1976). *A Point Energy and Mass Balance Model of a Snow Cover*. U.S. Department of Commerce, National Oceanic and Atmospheric Administration, National Weather Service, Office of Hydrology.

Andresen, C. G., Lawrence, D. M., Wilson, C. J., McGuire, A. D., Koven, C., Schaefer, K., et al. (2020). Soil moisture and hydrology projections of the permafrost region – a model intercomparison. *The Cryosphere (Online)*, *14*(2). https://doi.org/10.5194/tc-14-445-2020

Bartlett, P. A., McCaughey, J. H., Lafleur, P. M., & Verseghy, D. L. (2003). Modelling evapotranspiration at three boreal forest stands using the CLASS: tests of parameterizations for canopy conductance and soil evaporation. *International Journal of Climatology*, *23*(4), 427–451. https://doi.org/10.1002/joc.884

Bartsch, A., Balzter, H., & George, C. (2009). The influence of regional surface soil moisture anomalies on forest fires in Siberia observed from satellites. *Environmental Research Letters*, *4*(4), 045021. https://doi.org/10.1088/1748-9326/4/4/045021

Beven, K. (2006). A manifesto for the equifinality thesis. *Journal of Hydrology*, *320*(1), 18–36. https://doi.org/10.1016/j.jhydrol.2005.07.007

Beven, K., & Binley, A. (1992). The future of distributed models: Model calibration and uncertainty prediction. *Hydrological Processes*, *6*(3), 279–298. https://doi.org/10.1002/hyp.3360060305

Beven, K., & Binley, A. (2014). GLUE: 20 years on. *Hydrological Processes*, *28*(24), 5897–5918. https://doi.org/10.1002/hyp.10082

Beven, K., & Westerberg, I. (2011). On red herrings and real herrings: disinformation and information in hydrological inference. *Hydrological Processes*, *25*(10), 1676–1680. https://doi.org/10.1002/hyp.7963

Bieniek, P. A., Bhatt, U. S., Walsh, J. E., Rupp, T. S., Zhang, J., Krieger, J. R., & Lader, R. (2016). Dynamical Downscaling of ERA-Interim Temperature and Precipitation for Alaska. *Journal of Applied Meteorology and Climatology*, *55*(3), 635–654. https://doi.org/10.1175/JAMC-D-15-0153.1

Bladon, K. D., Silins, U., Landhäusser, S. M., & Lieffers, V. J. (2006). Differential transpiration by three boreal tree species in response to increased evaporative demand after variable retention harvesting. *Agricultural and Forest Meteorology*, *138*(1–4), 104–119. https://doi.org/10.1016/j.agrformet.2006.03.015

Blain, C. A., & Milly, P. C. D. (1991). Development and application of a hillslope hydrologic model. *Advances in Water Resources*, *14*(4), 168–174. https://doi.org/10.1016/0309-1708(91)90012-D

Blanken, P. D., Black, T. A., Yang, P. C., Neumann, H. H., Nesic, Z., Staebler, R., et al. (1997). Energy balance and canopy conductance of a boreal aspen forest: Partitioning overstory and understory components. *Journal of Geophysical Research: Atmospheres*, *102*(D24), 28915–28927. https://doi.org/10.1029/97JD00193

Bonan, G. B. (1993). Importance of leaf area index and forest type when estimating photosynthesis in boreal forests. *Remote Sensing of Environment*, *43*(3), 303–314. https://doi.org/10.1016/0034-4257(93)90072-6

Bonan, G. B., & Sirois, L. (1992). Air temperature, tree growth, and the northern and southern range limits to *Picea mariana*. *Journal of Vegetation Science*, *3*(4), 495–506. https://doi.org/10.2307/3235806

Bond-Lamberty, B., Wang, C., Gower, S. T., & Norman, J. (2002). Leaf area dynamics of a boreal black spruce fire chronosequence. *Tree Physiology*, *22*(14), 993–1001. https://doi.org/10.1093/treephys/22.14.993

Cable, J. M., Ogle, K., Bolton, W. R., Bentley, L. P., Romanovsky, V., Iwata, H., et al. (2014). Permafrost thaw affects boreal deciduous plant transpiration through increased soil water, deeper thaw, and warmer soils. *Ecohydrology*, *7*(3), 982–997. https://doi.org/10.1002/eco.1423

Cahoon, S. M. P., Sullivan, P. F., Brownlee, A. H., Pattison, R. R., Andersen, H.-E., Legner, K., & Hollingsworth, T. N. (2018). Contrasting drivers and trends of coniferous and deciduous tree growth in interior Alaska. *Ecology*. https://doi.org/10.1002/ecy.2223

Campbell, G. S., & Norman, J. M. (1998). *An Introduction to Environmental Biophysics*. Retrieved from https://doi.org/10.1007/978-1-4612-1626-1

Cannon, A. J. (2016). Multivariate Bias Correction of Climate Model Output: Matching Marginal Distributions and Intervariable Dependence Structure. *Journal of Climate*, *29*(19), 7045–7064. https://doi.org/10.1175/JCLI-D-15-0679.1

Carnell, R. (2019). lhs: Latin Hypercube Samples. (Version R package version 1.0.1). Retrieved from https://CRAN.R-project.org/package=lhs

Chappell, N. A., Franks, S. W., & Larenus, J. (1998). Multi-scale permeability estimation for a tropical catchment. *Hydrological Processes*, *12*(9), 1507–1523. https://doi.org/10.1002/(SICI)1099-1085(199807)12:9<1507::AID-HYP653>3.0.CO;2-J

Chegwidden, O. S., Nijssen, B., Rupp, D. E., Arnold, J. R., Clark, M. P., Hamman, J. J., et al. (2019). How Do Modeling Decisions Affect the Spread Among Hydrologic Climate Change Projections? Exploring a Large Ensemble of Simulations Across a Diversity of Hydroclimates. *Earth's Future*, *7*(6), 623–637. https://doi.org/10.1029/2018EF001047

Chen, J. M., Rich, P. M., Gower, S. T., Norman, J. M., & Plummer, S. (1997). Leaf area index of boreal forests: Theory, techniques, and measurements. *Journal of Geophysical Research: Atmospheres*, *102*(D24), 29429–29443. https://doi.org/10.1029/97JD01107

Da Veiga, S. (2015). Global sensitivity analysis with dependence measures. *Journal of Statistical Computation and Simulation*, *85*(7), 1283–1305. https://doi.org/10.1080/00949655.2014.945932

Dang, Q.-L., Margolis, H. A., Coyea, M. R., Sy, M., & Collatz, G. J. (1997). Regulation of branch-level gas exchange of boreal trees: roles of shoot water potential and vapor pressure difference. *Tree Physiology*, *17*(8–9), 521–535. https://doi.org/10.1093/treephys/17.8-9.521

Dettmann, U., Bechtold, M., Frahm, E., & Tiemeyer, B. (2014). On the applicability of unimodal and bimodal van Genuchten–Mualem based models to peat and other organic soils under evaporation conditions. *Journal of Hydrology*, *515*, 103–115. https://doi.org/10.1016/j.jhydrol.2014.04.047

Dobler, C., Hagemann, S., Wilby, R. L., & Stötter, J. (2012). Quantifying different sources of uncertainty in hydrological projections in an Alpine watershed. *Hydrology and Earth System Sciences*, *16*(11), 4343–4360. https://doi.org/10.5194/hess-16-4343-2012

Dunn, A. L., Barford, C. C., Wofsy, S. C., Goulden, M. L., & Daube, B. C. (2007). A long-term record of carbon exchange in a boreal black spruce forest: means, responses to interannual variability, and decadal trends. *Global Change Biology*, *13*(3), 577–590. https://doi.org/10.1111/j.1365-2486.2006.01221.x

Efstratiadis, A., & Koutsoyiannis, D. (2010). One decade of multi-objective calibration approaches in hydrological modelling: a review. *Hydrological Sciences Journal*, *55*(1), 58–78. https://doi.org/10.1080/02626660903526292

Endalamaw, A., Bolton, W. R., Young-Robertson, J. M., Morton, D., Hinzman, L., & Nijssen, B. (2017). Towards improved parameterization of a macroscale hydrologic model in a discontinuous permafrost boreal forest ecosystem. *Hydrol. Earth Syst. Sci.*, *21*(9), 4663–4680. https://doi.org/10.5194/hess-21-4663-2017

Feng, D., & Beighley, E. (2020). Identifying uncertainties in hydrologic fluxes and seasonality from hydrologic model components for climate change impact assessments. *Hydrology and Earth System Sciences*, *24*(5), 2253–2267. https://doi.org/10.5194/hess-24-2253-2020

Flerchinger, G. N. (2017). The Simultaneous Heat and Water (SHAW) Model: Technical Documentation. Technical Report NWRC 2017-02. Retrieved from https://pdfs.semanticscholar.org/4906/2b4ebd161d0df6179b113dd9b1e5abf7813f.pdf

Flerchinger, G. N., & Saxton, K. E. (1989). Simultaneous Heat and Water Model of a Freezing Snow-Residue-Soil System 1. Theory and Development. *Transactions of the ASABE*, *32*(2), 565–571.

Flerchinger, G. N., Seyfried, M. S., & Hardegree, S. P. (2006). Using Soil Freezing Characteristics to Model Multi-Season Soil Water Dynamics. *Vadose Zone Journal*, *5*(4), 1143–1153. https://doi.org/10.2136/vzj2006.0025

Fryer, J. L. (2014). *Picea mariana* (Fire Effects Information System). Online: U.S. Department of Agriculture, Forest Service, Rocky Mountain Research Station, Fire Sciences Laboratory. Retrieved from https://www.fs.fed.us/database/feis/plants/tree/picmar/all.html

Goldstein, G. H., Brubaker, L. B., & Hinckley, T. M. (1985). Water relations of white spruce (Picea glauca (Moench) Voss) at tree line in north central Alaska. *Canadian Journal of Forest Research*, *15*(6), 1080–1087. https://doi.org/10.1139/x85-176

Govind, A., Chen, J. M., McDonnell, J., Kumari, J., & Sonnentag, O. (2011). Effects of lateral hydrological processes on photosynthesis and evapotranspiration in a boreal ecosystem. *Ecohydrology*, *4*(3), 394–410. https://doi.org/10.1002/eco.141

Grayson, R. B., Moore, I. D., & McMahon, T. A. (1992). Physically based hydrologic modeling: 1. A terrain-based model for investigative purposes. *Water Resources Research*, *28*(10), 2639–2658. https://doi.org/10.1029/92WR01258

Grossnickle, S. C., & Blake, T. J. (1986). Environmental and physiological control of needle conductance for bare-root black spruce, white spruce, and jack pine seedlings on boreal cutover sites. *Canadian Journal of Botany*, *64*(5), 943–949. https://doi.org/10.1139/b86-126

Harp, D. R., Atchley, A. L., Painter, S. L., Coon, E. T., Wilson, C. J., Romanovsky, V. E., & Rowland, J. C. (2016). Effect of soil property uncertainties on permafrost thaw projections: a calibration-constrained analysis. *The Cryosphere*, *10*(1), 341–358. https://doi.org/10.5194/tc-10-341-2016

Heijmans, M. M. P. D., Arp, W. J., & Chapin, F. S. (2004). Carbon dioxide and water vapour exchange from understory species in boreal forest. *Agricultural and Forest Meteorology*, *123*(3–4), 135–147. https://doi.org/10.1016/j.agrformet.2003.12.006

Helbig, M., Waddington, J. M., Alekseychik, P., Amiro, B. D., Aurela, M., Barr, A. G., et al. (2020). Increasing contribution of peatlands to boreal evapotranspiration in a warming climate. *Nature Climate Change*, *10*(6), 555–560. https://doi.org/10.1038/s41558-020-0763-7

Houle, D., Bouffard, A., Duchesne, L., Logan, T., & Harvey, R. (2012). Projections of Future Soil Temperature and Water Content for Three Southern Quebec Forested Sites. *Journal of Climate*, *25*(21), 7690–7701. https://doi.org/10.1175/JCLI-D-11-00440.1

Iooss, B., & Lemaître, P. (2015). A Review on Global Sensitivity Analysis Methods. In G. Dellino & C. Meloni (Eds.), *Uncertainty Management in Simulation-Optimization of Complex Systems* (Vol. 59, pp. 101–122). Boston, MA: Springer US. https://doi.org/10.1007/978-1-4899-7547-8_5

Iooss, B., Veiga, S. D., Janon, A., & Pujol, G. (2020). sensitivity: Global Sensitivity Analysis of Model Outputs (Version R package version 1.22.0). Retrieved from https://CRAN.R-project.org/package=sensitivity

Iwata, H., Ueyama, M., Harazono, Y., Tsuyuzaki, S., Kondo, M., & Uchida, M. (2011). Quick Recovery of Carbon Dioxide Exchanges in a Burned Black Spruce Forest in Interior Alaska. *SOLA*, *7*, 105–108. https://doi.org/10.2151/sola.2011-027

Iwata, Hiroki, Harazono, Y., & Ueyama, M. (2010). Influence of Source/Sink Distributions on Flux–Gradient Relationships in the Roughness Sublayer Over an Open Forest Canopy Under Unstable Conditions. *Boundary-Layer Meteorology*, *136*(3), 391–405. https://doi.org/10.1007/s10546-010-9513-0

Jennings, K. S., Winchell, T. S., Livneh, B., & Molotch, N. P. (2018). Spatial variation of the rain–snow temperature threshold across the Northern Hemisphere. *Nature Communications*, *9*(1), 1148. https://doi.org/10.1038/s41467-018-03629-7

Jones, M.-F., Castonguay, M., Nasr, M., Ogilvie, J., Arp, P. A., & Bhatti, J. (2014). Modeling hydrothermal regimes and potential impacts of climate change on permafrost within the South

Mackenzie Plain, Northwest Territories, Canada. *Écoscience*, *21*(1), 21–33. https://doi.org/10.2980/21-1-3663

Körner, Ch. (1995). Leaf Diffusive Conductances in the Major Vegetation Types of the Globe. In E.-D. Schulze & M. M. Caldwell (Eds.), *Ecophysiology of Photosynthesis* (pp. 463–490). Berlin, Heidelberg: Springer Berlin Heidelberg. https://doi.org/10.1007/978-3-642-79354-7_22

Krishnan, P., Black, T. A., Barr, A. G., Grant, N. J., Gaumont-Guay, D., & Nesic, Z. (2008). Factors controlling the interannual variability in the carbon balance of a southern boreal black spruce forest. *Journal of Geophysical Research: Atmospheres*, *113*(D9). https://doi.org/10.1029/2007JD008965

Lader, R., Walsh, J. E., Bhatt, U. S., & Bieniek, P. A. (2017). Projections of Twenty-First-Century Climate Extremes for Alaska via Dynamical Downscaling and Quantile Mapping. *Journal of Applied Meteorology and Climatology*, *56*(9), 2393–2409. https://doi.org/10.1175/JAMC-D-16-0415.1

Lader, R., Walsh, J. E., Bhatt, U. S., & Bieniek, P. A. (2020). Anticipated changes to the snow season in Alaska: Elevation dependency, timing and extremes. *International Journal of Climatology*, *40*(1), 169–187. https://doi.org/10.1002/joc.6201

Lamhamedi, M., & Bernier, P. (1994). Ecophysiology and field performance of black spruce (Picea mariana): a review. *Annales Des Sciences Forestières*, *51*(6), 529–551. https://doi.org/10.1051/forest:19940601

Launiainen, S., Guan, M., Salmivaara, A., & Kieloaho, A.-J. (2019). Modeling boreal forest evapotranspiration and water balance at stand and catchment scales: a spatial approach. *Hydrology and Earth System Sciences*, *23*(8), 3457–3480. https://doi.org/10.5194/hess-23-3457-2019

Li, X., Xiao, Q., Niu, J., Dymond, S., McPherson, E. G., van Doorn, N., et al. (2017). Rainfall interception by tree crown and leaf litter: An interactive process. *Hydrological Processes*, *31*(20), 3533–3542. https://doi.org/10.1002/hyp.11275

Link, T. E., Flerchinger, G. N., Unsworth, M., & Marks, D. (2004). Simulation of Water and Energy Fluxes in an Old-Growth Seasonal Temperate Rain Forest Using the Simultaneous Heat and Water (SHAW) Model. *Journal of Hydrometeorology*, *5*(3), 443–457. https://doi.org/10.1175/1525-7541(2004)005<0443:SOWAEF>2.0.CO;2

Liu, H., & Lennartz, B. (2019). Hydraulic properties of peat soils along a bulk density gradient-A meta study. *Hydrological Processes*, *33*(1), 101–114. https://doi.org/10.1002/hyp.13314

L.O. Safford, John C. Bjorkbom, & John C. Zasada. (1990). Betula papyifera Marsh. Paper Birch. In *Silvics of North America* (Vol. 2, pp. 158–171). Washington, DC: U.S. Department of Agriculture, Forest Service.

Ludwig, R., May, I., Turcotte, R., Vescovi, L., Braun, M., Cyr, J.-F., et al. (2009). The role of hydrological model complexity and uncertainty in climate change impact assessment. *Advances in Geosciences*, *21*, 63–71. https://doi.org/10.5194/adgeo-21-63-2009

Maire, V., Wright, I. J., Prentice, I. C., Batjes, N. H., Bhaskar, R., van Bodegom, P. M., et al. (2015). Global effects of soil and climate on leaf photosynthetic traits and rates: Effects of soil and climate on photosynthetic traits. *Global Ecology and Biogeography*, *24*(6), 706–717. https://doi.org/10.1111/geb.12296

Marshall, A., Link, T., Flerchinger, G., Nicolsky, D., & Lucash, M. (2020). *Ecohydrologic modeling in deciduous boreal forest: Model evaluation for application in non-stationary climates* (preprint). Preprints. https://doi.org/10.22541/au.160414217.73787642/v1

Melvin, A. M., Mack, M. C., Johnstone, J. F., David McGuire, A., Genet, H., & Schuur, E. A. G. (2015). Differences in Ecosystem Carbon Distribution and Nutrient Cycling Linked to Forest Tree Species Composition in a Mid-Successional Boreal Forest. *Ecosystems*, *18*(8), 1472–1488. https://doi.org/10.1007/s10021-015-9912-7

Mendoza, P. A., Clark, M. P., Mizukami, N., Gutmann, E. D., Arnold, J. R., Brekke, L. D., & Rajagopalan, B. (2016). How do hydrologic modeling decisions affect the portrayal of climate change impacts?: Subjective Hydrologic Modelling Decisions in Climate Change Impacts. *Hydrological Processes*, *30*(7), 1071–1095. https://doi.org/10.1002/hyp.10684

Menne, M. J., Durre, I., Korzeniewski, B., McNeal, S., Thomas, K., Yin, X., et al. (2012). Global Historical Climatology Network - Daily (GHCN-Daily). *NOAA National Climatic Data Center*, *Version 3*. https://doi.org/10.7289/V5D21VHZ

Murray, M., Soh, W. K., Yiotis, C., Spicer, R. A., Lawson, T., & McElwain, J. C. (2020). Consistent Relationship between Field-Measured Stomatal Conductance and Theoretical Maximum Stomatal Conductance in C3 Woody Angiosperms in Four Major Biomes. *International Journal of Plant Sciences*, *181*(1), 142–154. https://doi.org/10.1086/706260

National Cooperative Soil Survey. (2020). *National Cooperative Soil Survey Soil Characterization Database*. Retrieved from http://ncsslabdatamart.sc.egov.usda.gov/

Pianosi, F., Beven, K., Freer, J., Hall, J. W., Rougier, J., Stephenson, D. B., & Wagener, T. (2016). Sensitivity analysis of environmental models: A systematic review with practical workflow. *Environmental Modelling & Software*, *79*, 214–232. https://doi.org/10.1016/j.envsoft.2016.02.008

Ranney, T. G., & Peet, M. M. (1994). Heat Tolerance of Five Taxa of Birch (Betula): Physiological Responses to Supraoptimal Leaf Temperatures. *Journal of the American Society for Horticultural Science*, *119*(2), 243–248. https://doi.org/10.21273/JASHS.119.2.243

Salmon, Y., Lintunen, A., Dayet, A., Chan, T., Dewar, R., Vesala, T., & Hölttä, T. (2020). Leaf carbon and water status control stomatal and nonstomatal limitations of photosynthesis in trees. *New Phytologist*, *226*(3), 690–703. https://doi.org/10.1111/nph.16436

Saltelli, A., Aleksankina, K., Becker, W., Fennell, P., Ferretti, F., Holst, N., et al. (2019). Why so many published sensitivity analyses are false: A systematic review of sensitivity analysis practices. *Environmental Modelling & Software*, *114*, 29–39. https://doi.org/10.1016/j.envsoft.2019.01.012

Serbin, S. P., Ahl, D. E., & Gower, S. T. (2013). Spatial and temporal validation of the MODIS LAI and FPAR products across a boreal forest wildfire chronosequence. *Remote Sensing of Environment*, *133*, 71–84. https://doi.org/10.1016/j.rse.2013.01.022

Subin, Z. M., Koven, C. D., Riley, W. J., Torn, M. S., Lawrence, D. M., & Swenson, S. C. (2012). Effects of Soil Moisture on the Responses of Soil Temperatures to Climate Change in Cold Regions. *Journal of Climate*, *26*(10), 3139–3158. https://doi.org/10.1175/JCLI-D-12-00305.1

Teufel, B., & Sushama, L. (2019). Abrupt changes across the Arctic permafrost region endanger northern development. *Nature Climate Change*, *9*(11), 858–862. https://doi.org/10.1038/s41558-019-0614-6

Ueyama, M., Harazono, Y., Kim, Y., & Tanaka, N. (2009). Response of the carbon cycle in sub-arctic black spruce forests to climate change: Reduction of a carbon sink related to the sensitivity of heterotrophic respiration. *Agricultural and Forest Meteorology*, *149*(3), 582–602. https://doi.org/10.1016/j.agrformet.2008.10.011

Ueyama, M., Iwata, H., Nagano, H., Tahara, N., Iwama, C., & Harazono, Y. (2019). Carbon dioxide balance in early-successional forests after forest fires in interior Alaska. *Agricultural and Forest Meteorology*, *275*, 196–207. https://doi.org/10.1016/j.agrformet.2019.05.020

Van Pelt, R. (2007). *Identifying Mature and Old Forests in Western Washington* (p. 104). Olympia, WA: Washington State Department of Natural Resources.

Viereck, L. A., Dyrness, C. T., Cleve, K. V., & Foote, M. J. (1983). Vegetation, soils, and forest productivity in selected forest types in interior Alaska. *Canadian Journal of Forest Research*, *13*(5), 703–720. https://doi.org/10.1139/x83-101

Wang, J. R., Zhong, A. L., Comeau, P., Tsze, M., & Kimmins, J. P. (1995). Aboveground biomass and nutrient accumulation in an age sequence of aspen (Populus tremuloides) stands in the Boreal White and Black Spruce Zone, British Columbia. *Forest Ecology and Management*, *78*(1), 127–138. https://doi.org/10.1016/0378-1127(95)03590-0

Wilby, R. L. (2005). Uncertainty in water resource model parameters used for climate change impact assessment. *Hydrological Processes*, *19*(16), 3201–3219. https://doi.org/10.1002/hyp.5819

Wilks, D. S. (2016). "The Stippling Shows Statistically Significant Grid Points": How Research Results are Routinely Overstated and Overinterpreted, and What to Do about It. *Bulletin of the American Meteorological Society*, *97*(12), 2263–2273. https://doi.org/10.1175/BAMS-D-15-00267.1

Yarie, J., & van Cleve, K. (2010). Long-term monitoring of climatic and nutritional affects on tree growth in interior Alaska. *Canadian Journal of Forest Research. 40: 1325-1335*, *40*, 1325–1335.

Yarie, John, & Billings, S. (2002). Carbon balance of the taiga forest within Alaska: Present and future. *Canadian Journal of Forest Research*, *32*, 757–767. https://doi.org/10.1139/x01-075

Yarie, John, Kane, E., & Mack, M. (2007). Aboveground Biomass Equations for the Trees of Interior Alaska. *AFES Bulletin*, *115*, 16.

Zhang, Y., Carey, S. K., Quinton, W. L., Janowicz, J. R., Pomeroy, J. W., & Flerchinger, G. N. (2010). Comparison of algorithms and parameterisations for infiltration into organic-covered permafrost soils. *Hydrol. Earth Syst. Sci.*, *14*(5), 729–750. https://doi.org/10.5194/hess-14-729-2010

Zhang, Y., Cheng, G., Li, X., Han, X., Wang, L., Li, H., et al. (2013). Coupling of a simultaneous heat and water model with a distributed hydrological model and evaluation of the combined model in a cold region watershed. *Hydrological Processes*, *27*(25), 3762–3776. https://doi.org/10.1002/hyp.9514

Zwieback, S., Westermann, S., Langer, M., Boike, J., Marsh, P., & Berg, A. (2019). Improving Permafrost Modeling by Assimilating Remotely Sensed Soil Moisture. *Water Resources Research*, *55*(3), 1814–1832. https://doi.org/10.1029/2018WR023247